

SOME VARIATIONS IN PROPERTIES OF COAL MACERALS ELUCIDATED BY DENSITY GRADIENT SEPARATION*

Gary R. Dyrkacz, C. A. A. Bloomquist, L. Ruscic, and
E. Philip Horwitz

Chemistry Division, Argonne National Laboratory
Argonne, Illinois 60439

INTRODUCTION

Our recent development of a new procedure for the density separation of macerals offers a method for obtaining high resolution separation of the maceral groups: exinite, vitrinite, and inertinite, and can further resolve individual maceral types, e.g., sporinite (1,2). The procedure utilizes well-known techniques of density gradient centrifugation (DGC) to separate the coal into its components in a continuous aqueous CsCl density gradient. This results in a series of bands representing the density variations in maceral groups and maceral types. The gradient is then divided into convenient size fractions, the coal in each fraction is isolated and micropetrographic analyses are performed on selected fractions. In addition to providing pure materials for further work, a density fingerprint of a coal is produced. The observed changes in density are related in a complex way to the chemical structure of the coal or maceral (3). In order to better understand the chemical variations occurring in coal macerals we have examined the ultimate analysis of selected density fractions separated from the same coal.

EXPERIMENTAL

Separation

The basic procedures for DGC separation of macerals with advantages and disadvantages has been discussed previously (1,2). To summarize, the coal is ground to ~3 micron average particle size, chemically demineralized and separated on a density gradient. The gradient is then divided into fractions of ~0.01 g/cc range and each fraction is then filtered, washed, and dried.

Analysis

Because of the small samples often generated, ultimate analysis of selected density fractions was performed with a Perkin-Elmer 240 C, H, N Analyzer using a modified burn procedure which includes increasing the time of burn and the amount of O₂ used in the burn. Good correlation ($r^2 = .98$) with ASTM methods was found for a range of coals from sub-bituminous to anthracites.

RESULTS AND DISCUSSION

All the coals used here were obtained from the Pennsylvania State University Coal Data Base. The data for the coals are given in Table I. The separation of all these coals was performed in the same way and all the coals were resolved to the same degree. We have previously published detailed separation data on the high volatile B bituminous coal, PSOC-106, which gave good yields of all three maceral groups (1,3). The exinite in this coal is mainly sporinite, while the inertinite is mainly semi-fusinite. Figure 1a shows the distribution of the pure maceral particles as a function of density for PSOC-106. Pure maceral particles refer to those particles which by optical microscopy are composed of only one maceral species. Figure 1b shows the corresponding atomic ratios H/C, S/C, N/C, and O/C.

*Work performed under the auspices of the Office of Basic Energy Sciences, Division of Chemical Sciences, U. S. Department of Energy, under Contract W-31-109-Eng-38.

The selected fractions analyzed represent density fractions consisting of at least 88% (vol.) of a single maceral species. The lines connecting sets of points between maceral groups must not be taken literally. These intermediate regions consist of particles with two or more macerals composing a single particle or two distinct populations of pure maceral particles. Thus, whether or not the connecting lines between maceral groups represent the atomic value in that region, their only purpose for this discussion is to aid the eye in following trends between maceral groups.

The H/C ratio exhibits a very large range of values over the entire coal: from 1.13 at the lowest density monitored to 0.48 at the highest density. The S/C ratios follow a similar trend: with the highest sulfur values in exinites and the lowest in inertinites. These sulfur values represent almost all organic sulfur since pyritic sulfur has been eliminated by the separation procedure. The S/C data is consistent with data found by an 'in situ' method of sulfur analysis in coal (4). Because of the nature of the separation method we can also see significant variations not only between maceral groups, but within each maceral group. Figure 2 is an attempt to provide some idea of the magnitude of variation that exists in the H/C ratio in the three maceral groups. The distributions are incomplete because of overlapping of maceral bands or composite maceral particles which give unreliable data. Table II represents the range of H/C values for each band and combined with previous ^{13}C with solid probe nmr data for f_a , shows the ring index or number of rings per 100 carbon atoms. The data for 50% of the coal refers to the coal centered around the peak value. The ring index includes all aromatic, aliphatic, and heterocyclic rings. The number of rings per 100 carbons is roughly the same for all the maceral groups and indicates, as expected, that they are all highly condensed species. However, the ratio of aromatic to aliphatic rings increases dramatically from exinites to inertinites. Exinite tends to exhibit wide variations in its composition, while vitrinite and inertinite are somewhat less variable. In all cases, though, the indications are that substantial variations in each maceral group are being observed by the density separation method. The oxygen and nitrogen data also show strong variations within the exinites and vitrinites, while inertinites do not.

In Figure 3 we have used the graphical densimetric method to show how the ring index varies with the density of the macerals (5). As can be seen the data parallels the increase in aromaticity.

The change in atomic ratios are not unique to the particular coal PSOC-106. Figures 4a and 4b show data on three more bituminous coals which contain substantial amounts of all three maceral groups. (The very high H/C value of 1.4 for PSOC-297 is due to alginite in this coal.) Although all the coals exhibit their own character in the magnitude and range of the H/C values, they all show significant chemical changes across each maceral band in a similar manner to PSOC-106. Similar data also holds for coals that contain $\pm 95\%$ vitrinite.

What do these variations represent? There are a number of factors which can be invoked to explain the changes observed. Each of the three major maceral groups is composed of sub-macerals (maceral types). Exinite is composed of the maceral types: sporinite, resinite, alginite, cutinite. Since the source materials for each maceral type had different chemical structures some artifact of these differences would be expected to remain. This is one source of variation. Moreover, within a single maceral type itself significant petrographic changes can be observed. For example, different spore species show different fluorescence color, and collinite and semi-fusinite can have broad reflectance ranges within a coal. All these microscopically observable changes suggest differences in chemical structure. Qualitatively, we do see regular variations in fluorescence and reflectance across the maceral bands. It is apparent that density gradient centrifugation can, to some extent, isolate these physical and chemical variations and, in a sense, provide more

homogeneous materials. However, the chemical variations we see by DGC have to be considered as lower limits of the chemical heterogeneity expected for coal. Since we are still dealing with discrete particles, its density may still be a weighted average of the maceral variants comprising the particle, even though these variants are below optical resolution. Further grinding may separate these variants, but problems of mechanochemistry and surface problems may then become significant.

CONCLUSIONS

Substantial variation in the chemical behavior of macerals has been shown for a number of coals. Density gradient techniques can provide better defined, more homogeneous materials as well as provide a lower limit on the heterogeneity.

REFERENCES

1. Dyrkacz, Gary R. and Horwitz, E. Philip, *Fuel*, 61, 3 (1982).
2. Dyrkacz, Gary R., Bloomquist, C. A. A., and Horwitz, E. Philip, *Separation Science and Technology*, 16, 1571 (1981).
3. Van Krevelen, D. W., 'Coal', Elsevier, 1961, p. 315.
4. Raymond, R., *International Conference on Coal Science, Proceedings, Dusseldorf, 1981*, p. 857.
5. Van Krevelen, D. W. and Chermin, H. H. G., *Fuel*, 33, 338 (1954).
6. Pugmire, R. J., Zilm, K. W., Woolfenden, W. R., Grant, D. M., Dyrkacz, G. R., Bloomquist, C. A. A., and Horwitz, E. P., *Jour. Org. Geochem.*, in press.

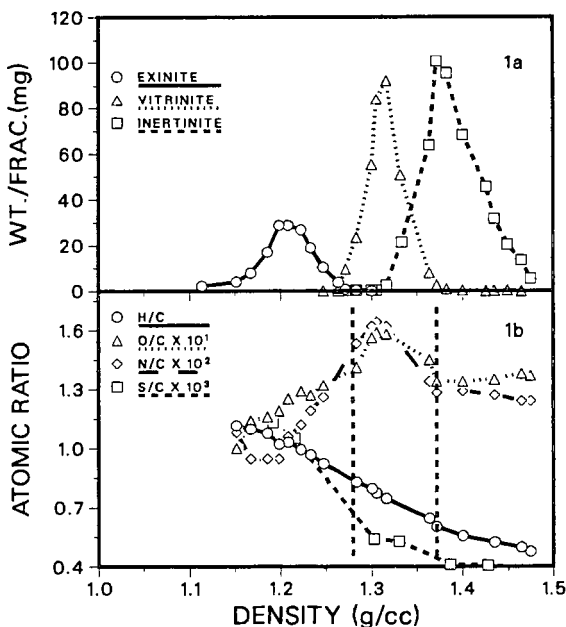


Figure 1a. Pure maceral distribution of PSOC-106.
1b. Variations of atomic parameters.

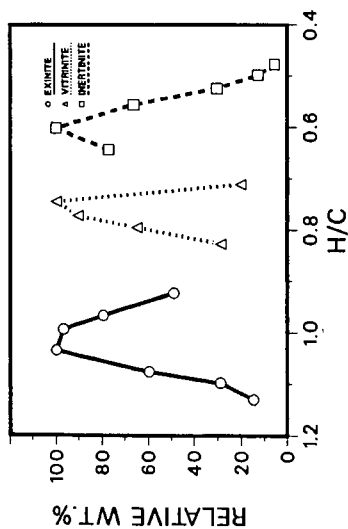


Figure 2. Distribution of coal macerals in PSOC-106 as a function of H/C ratio.

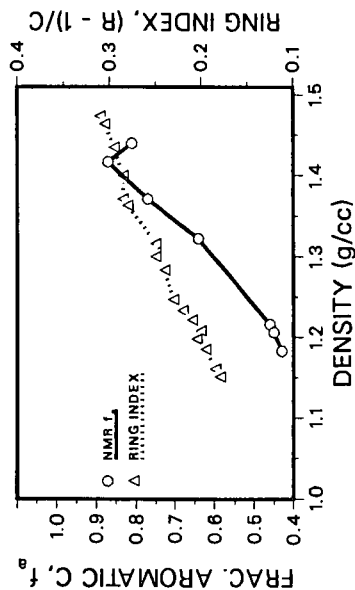


Figure 3. Variation of f_a and ring index with density in PSOC-106.

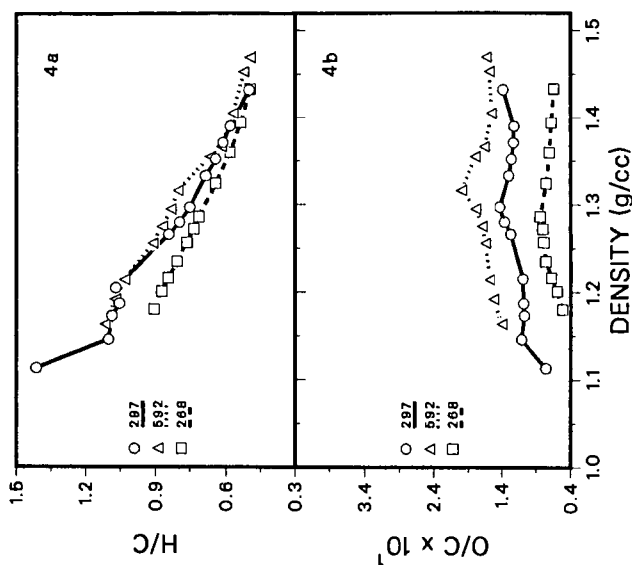


Figure 4a. Variation of H/C ratio with density.
4b. Variation of O/C ratio with density.

COMPUTERIZED PYROLYSIS MASS SPECTROMETRY OF COAL MACERAL CONCENTRATES

Henk L.C. Meuzelaar, Alice M. Harper and Ronald J. Pugmire

University of Utah, Salt Lake City, Utah 84112

INTRODUCTION

A few pyrolysis mass spectra of purified coal maceral concentrates have appeared in the literature [1-4] showing the presence of more or less pronounced differences between the spectra of vitrinites, fusinites, sporinites and alginites. However, these studies did not attempt to distinguish between the possible effects of rank or depositional environment on the spectra and the more basic structural differences between maceral types.

Recently, the feasibility of distinguishing between these effects was demonstrated by Meuzelaar *et al.* [5,6] in a study of over 100 Rocky Mountain coal samples by Curie-point pyrolysis mass spectrometry (Py-MS) in combination with computerized multivariate statistical analysis of the data. In the present study, the same analytical approach is used to characterize a set of 30 selected maceral concentrates.

EXPERIMENTAL

The maceral concentrates analyzed are listed in Table I. Seventeen samples originated from the maceral collection of the British National Coal Board and had been prepared by the sink/flotation method. Most of these were obtained through Dr. Given at Penn State University who redistributed these samples to different groups as part of a cooperative study [7]. Thirteen maceral concentrate fractions were prepared from two US coals by the cesium chloride gradient centrifugation method [8].

Samples were ground to 300 mesh under liquid nitrogen and 4 mg aliquots were suspended in 1 ml of methanol. Two 5 microliter drops of this suspension were coated on the ferromagnetic filaments used in Curie-point pyrolysis. A detailed description of the sample preparation and Curie-point Py-MS methods has been given elsewhere [4,6]. The Py-MS system used was an Extranuclear 5000-1 Curie-point pyrolysis MS system based on a quadrupole mass spectrometer. Experimental conditions were as follows: sample weight 20 μ g, Curie-point temperature 610°C, temperature rise time 5 s, total heating time 10 s, electron impact ionization energy 12 eV, mass range m/z 20-260, scanning speed 1000 amu/s, total scanning time 25 s. All samples were analyzed in triplicate. Data processing involved the use of computerized signal averaging followed by spectrum calibration, normalization and scaling procedures. Multivariate statistical analysis, e.g. factor analysis, procedures involved the use of SPSS [9] and ARTHUR [10] program packages.

RESULTS AND DISCUSSION

Three pyrolysis mass spectra averaged over all vitrinites, inertinites and exinites (sporinites) respectively are shown in Figure 1. The overall pattern of each maceral group agrees quite well with the spectra published by other authors [1-4], with vitrinites showing prominent phenolic series, fusinites being dominated by aromatic hydrocarbon signals and sporinites showing marked alkene peaks. More subtle differences - the significance of which can only be appreciated with the help of computerized data analysis techniques - will be discussed later.

Figure 2 shows a scatter plot of m/z 110 vs. 124, two peaks known to provide a direct measure of rank in high volatile bituminous coals [5,6] and believed to represent dihydroxybenzenes and methyl-dihydroxybenzenes respectively. The peak intensities in Figure 2 indeed appear to correspond more or less directly with

carbon content and to be largely independent of maceral type. In other words, if carbon content is accepted as a measure of the rank of whole coals then a plot of m/z 110 vs. 124 will reflect this rank measure in spite of possible differences in maceral composition. However, it hardly needs to be pointed out that the large differences in carbon content between macerals from the same coal (see Table I) illustrate the inadequacy of using carbon content as a coalification parameter for coals with markedly different maceral compositions.

Figure 3 shows a scatter plot of the peak intensities of m/z 34 vs. 122, two peaks known to be influenced strongly by differences in depositional environment [5,6] and thought to represent hydrogen sulfide and C_2 -alkylphenols respectively. In a previous study of whole coals from the US Rocky Mountain coal province the ion intensity at m/z 34 was found to correlate strongly with organic sulfur content. However, in this study insufficient data were available on organic sulfur content to attempt such a correlation. Nevertheless a crude correlation appears to exist with total sulfur content. In agreement with Py-MS studies on whole coals [5] the alkylphenol peak intensities at m/z 122 show a rough negative correlation with rank. Nevertheless, four of the British vitrinites show much higher peak intensity values at m/z 122 than the US vitrinites of comparable rank. This is not surprising, since differences in hydroxyl content between coals from different depositional environments have also been reported [11].

Finally, the high intensity of m/z 122 in the Dunsil seam inertinite, compared to the other inertinites should be noted. This is probably due to the relatively low rank of the Dunsil inertinite as well as to the fact that this sample is composed largely of semifusinite. All semifusinite-rich samples included in this study (see Table I) exhibit mass spectral patterns which tend to be intermediate between fusinites and vitrinites (compare also the two Ballarat seam samples in Figure 3) which is in agreement with presently accepted views on the origin of semifusinites from partly charred wood [12].

In view of the presence of strongly correlating series of homologous ions in all maceral spectra, as shown in Figure 1, factor analysis was performed to reduce the apparent dimensionality of the data and to bring out the major underlying chemical tendencies. The K-L plot in Figure 4 was obtained while using 80 mass peaks with highest ratio's for "between category" and "within category" variance (with each set of three replicate spectra per sample serving as a separate category). Figure 4 shows a clear separation between the three different maceral groups, with vitrinites occupying an intermediate position between fusinites and exinites. The density gradient centrifugation samples of the two US coals blend in amazingly well with the corresponding British macerals. Moreover, factor I appears to show a positive correlation with differences in sample density.

To help explain the differences in chemical composition between the three maceral groups causing the separation in Figure 4 a spectrum of the first factor, calculated according to a procedure described by Windig *et al.* [13], is shown in Figure 5. The positive component of this factor spectrum is explained by peaks with relatively high intensities in inertinites (compare with Figure 4) and is thought to represent polynuclear aromatic series with rather pronounced degrees of alkyl substitution, e.g. biphenyls and/or acenaphthenes, phenanthrenes and/or anthracenes, fluorenes, etc. The high intensity of the residual methanol solvent peak groups at m/z 30-33 in inertinites may well reflect the long known correlation between the methanol absorption capacity of a coal and its degree of coalification [14]. The negative component of the factor spectrum - largely explained by peaks with relatively high intensities in the sporinite samples - shows a distinct peak pattern which we interpret as representing (poly)isoprenoids and/or related polyenic compounds. This pattern is found in all five sporinites, in spite of differences in origin, coalification stage and preparation technique. Moreover, in contrast with the more or less completely saturated or aromatized isoprenoid skeletons reported in the extractable fractions of coals and shales [15], these isoprenoid fragments liberated by Curie-point pyrolysis appear to possess a degree of unsaturation consistent with that found in many naturally occurring isoprenoids. Whether these polyenic signals are derived from carotenoid moieties in sporopollenin

[16] or perhaps from some type of fossilized natural rubber, remains open to speculation at this point. Selected peak intensities at m/z 122 and 288, representing the positive (inertinite) and negative (sporinite) components of factor I respectively, are shown in Figure 6.

Although the positive portion of the factor spectrum of factor II (not shown) might be expected to provide peak patterns characteristic of vitrinites, few if any such peaks are found. In fact, factor II is dominated by an as yet unexplained series of peaks loading on the negative component and thus representing compounds which are characteristically low in vitrinites as compared to inertinites and exinites.

It may be concluded that Curie-point pyrolysis mass spectrometry in combination with multivariate statistical analysis provides valuable information on the specific chemical characteristics of coal maceral concentrates as well as on the influence of depositional environment and coalification processes. The results obtained appear to agree well with generally accepted views on the chemical nature and origin of coal macerals. Perhaps the most important new finding of this study is the presence of distinct peak patterns in sporinites which appear to represent more or less intact (poly)isoprenoid and/or related polyenic hydrocarbon moieties. More detailed accounts of these studies are being published elsewhere [6].

TABLE I
MACERAL CONCENTRATES ANALYZED

NCB SINK/FLOTATION CONCENTRATES									
Sample			Maceral Composition (%)			Elemental Composition			
#	Code	Seam (Colliery)	VITRIN	INERT	LIPT	% C	% H	% O	% N % S _t
1	T	Dunsil (Teversal)	98	1	1	81.5	5.1	10.8	2.1 1.4
2	T	ibid	6	93*	tr.	87.7	3.9	6.9	1.1 1.6
3	M	Barnsley (Markham)	3	9	8B	82.2	7.4	7.3	1.1 1.9
4	M	ibid	98	2	tr.	82.2	5.5	9.3	1.9 1.3
5	M	ibid	6	92**	1	91.6	3.6	4.1	0.4 1.2
6	W	Wheatley Lime (Woolley)	96	1	3	87.9	6.9	3.0	1.1 1.2
7	W	ibid	3	9	8B	86.5	5.6	4.9	1.8 1.4
8	A	Silkstone (Aldwarke)	0	5	95	87.2	7.4	3.6	1.2 0.7
9	A	ibid	98	1	1	86.9	5.4	4.2	1.8 1.1
10	A	ibid	5	96*	-	92.1	3.7	3.1	0.7 0.4
11	R	Ballarat (Roddymoor)	96	3	1	88.8	5.3	3.6	1.7 0.7
12	Ra	ibid	2	97	-	93.9	3.5	1.4	0.5 0.8
13	Rb	ibid	14	85*	1	91.9	4.3	3.1	0.3 0.5
14	C	Gellideg (Coegnant)	89	11	0	91.4	4.6	1.9	1.6 0.6
15	C	ibid	34	66	0	92.3	4.2	1.9	1.1 0.6
16	P	Beeston (Peckfield)	"exinite"; density 1.22 g/cm ³						
17	P	ibid	"inertinite"; density 1.44 g/cm ³						
U OF U DENSITY GRADIENT FRACTIONS									
Sample			Seam (Coal Field)			Density (g/cm ³)		Maceral Type	
#	Code								
18	E1	Upper Elkhorn (E. Appalachian)			1.17		SPORIN		
19	E2	ibid			1.26		VITRIN		
20	E3	ibid [PSOC 2]			1.29		VITRIN		
21	E4	ibid [85.6 %C]			1.30		VITRIN		
22	E5	ibid			1.32		INERT***		
23	E6	ibid			1.36		INERT***		
24	S1	Dakota (San Juan River)			1.23		VITRIN		
25	S2	ibid			1.25		VITRIN		
26	S3	ibid			1.26		VITRIN		
27	S4	ibid [PSOC 858]			1.27		VITRIN		
28	S5	ibid [84.2 %C]			1.30		VITRIN		
29	S6	ibid			1.32		SFUSIN		
30	S7	ibid			1.38		SFUSIN		

* semifusinite

** equal amounts of fusinite and semifusinite

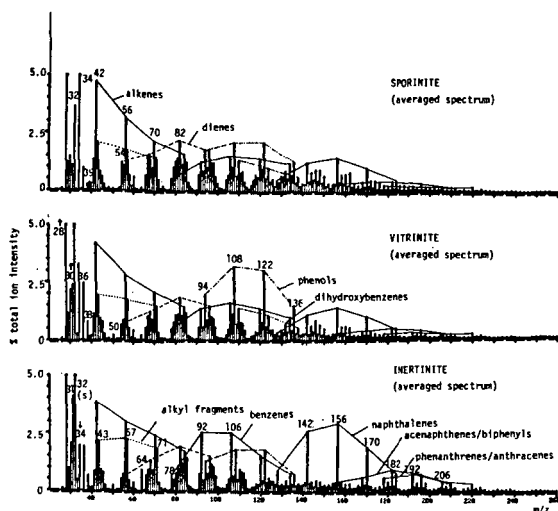
*** the parent coal (PSOC 2) contains approximately equal amounts of fusinite, semifusinite, macrinite and micrinite.

ACKNOWLEDGEMENTS

The generous help of the British National Coal Board and the Pennsylvania State University in obtaining well characterized maceral samples is gratefully acknowledged. Furthermore, the authors are indebted to Dr. J. Karas for preparing the gradient centrifugation samples and to D.J. Davis and K.H. Wong for performing these analyses. The research reported here was sponsored by DOE grant DE FG22-80PC30242 and by matching funds from the State of Utah.

REFERENCES

1. Van Graas, G., de Leeuw, J.W. and Schenck, P.A., in *Advances in Organic Geochemistry*, A.G. Douglas and J.R. Maxwell, eds., Pergamon Press (Oxford), 1979, p. 485.
2. Larter, S.R., Ph.D. Thesis, University of Newcastle upon Tyne, England, 1978.
3. Allan, J. and Larter, S.R., Proc. 10th Int. Meeting on Organic Geochemistry, Bergen (Norway), September 1981 (in press).
4. Meuzelaar, H.L.C., Haverkamp, J. and Hileman, F.D., *Curie-point Pyrolysis Mass Spectrometry of Recent and Fossil Biomaterials; Compendium and Atlas*, Elsevier, Amsterdam, (1982).
5. Meuzelaar, H.L.C., Harper, A.M. and Given, P.H., Proc. 5th ROMOCO Symp., UGMS Bulletin 118, 1982, p. 192.
6. Meuzelaar, H.L.C., Harper, A.M., Hill, G.R., Futrell, J.H., Davis, D.J. and Metcalf, G.S., Final report to DOE (Grant #DE-FG22-80PC30242) 1982.
7. Given, P.H., in *Organic Geochemistry and Chemistry and Coal Macerals for Advances in Chemistry Series*, J.W. Larsen (ed.) to be published.
8. Dyrkacz, G.R., Bloomquist, C.A.A., Winans, R.E. and Horwitz, E.P., Proc. Int. Conf. Coal Science, Dusseldorf, Verlag Gluckauf GmbH, Essen, 1981, p. 34.
9. Nie, N.H., Hull, C.H., Jenkins, J.G., Steinbrenner, K. and Bent, D.H., *Statistical Package for the Social Sciences* (2nd Ed.), McGraw-Hill, N.Y., 1975.
10. Harper, A.M., Duewer, D.L., Kowalski, B.R., Fasching, J.L., in *Chemometrics: Theory and Application*, B.R. Kowalski (ed.), Washington, D.C., ACS Symp. Series No. 52, 1977, p. 14.
11. Yarzab, R.F., Abdel-Baset, Z., and Given, P.H., *Geochem. et Cosmochim. Acta*, 43:281 (1979).
12. Teichmuller, M., Teichmuller, R., in *Stach's Textbook of Coal Petrology*, E. Stach, G.H. Taylor, M-Th Mackowsky, D. Chandra, M. Teichmuller and R. Teichmuller (eds.), Gebruder Borntraeger, Berlin, 1975, p. 5.
13. Windig, W., Kistemaker, P.G., Haverkamp, J. and Meuzelaar, H.L.C., *J. Anal. Appl. Pyrol.*, 2:7 (1980).
14. Van Krevelen, D.W., *Coal*, Elsevier, Amsterdam, 1961.
15. Gallegos, E.J., in *Developments in Petroleum Science*, Vol. 5, T.F. Yen and G.V. Chilingarian (eds.), Elsevier Scientific Pub. Co., Amsterdam, 1976.
16. Brooks, J. and Shaw G., in *Sporopollenin*, J. Brooks, P.R. Grant, M. Muir, P. van Gijzel and G. Shaw (eds.), Academic Press, London, 1971, p. 351.



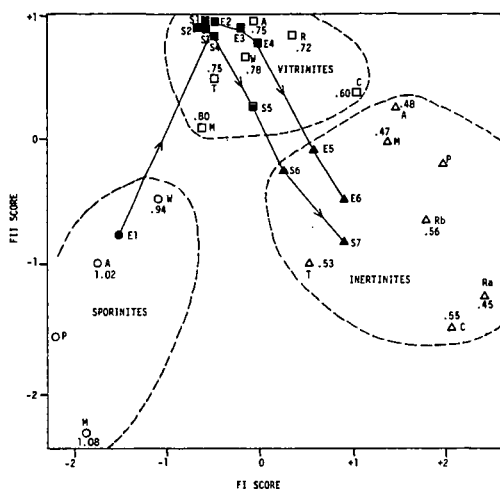


Figure 4. Karhunen Loeve plot of the first two factor scores. For explanation of symbols and codes see Figure caption 2 and Table I. US density gradient fractions are connected by arrows in order of increasing density. Numerical values ranging from .45 (Ballarat inertinite a) to 1.08 (Barnsley exinite) represent atomic H/C ratio's. Note positive correlation of factor I with density and negative correlation with H/C ratio.

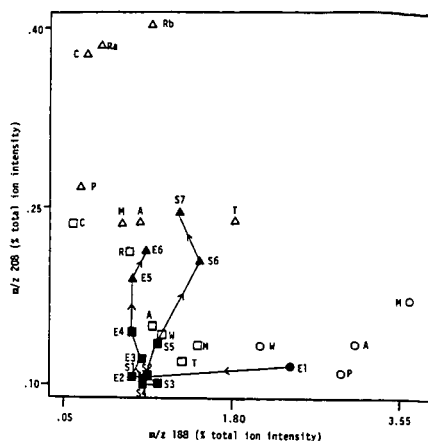


Figure 6. Scatter plot of ion intensities at m/z 188 and 208 believed to represent $C_{14}H_{20}$ polyenic and $C_{16}H_{16}$ polynuclear aromatic hydrocarbon compounds respectively. For explanation of symbols and codes see Figure caption 2 and Table I. Comparison with Figure 5 shows that m/z 208 is prominent in the positive component of Factor I whereas m/z 188 is one of the highest mass peaks in the negative component.

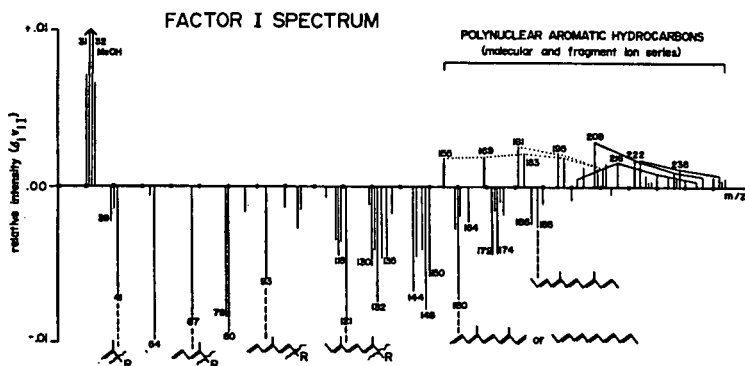


Figure 5. Factor spectrum representing factor I in Figure 4. Note marked simplification of spectral patterns as compared to Figure 1. Chemical labels are examples of possible structures only.

APPLICATION OF 2-D AND DIPOLAR DEPHASING ^{13}C NMR TECHNIQUES
TO THE STUDY OF STRUCTURAL VARIATIONS IN COAL MACERALS

Ronald J. Pugmire, Warner R. Woolfenden, Charles L. Mayne
Jirina Karas, and David M. Grant

University of Utah
Salt Lake City, Utah 84112

INTRODUCTION

Coal has been described as an organic rock. In order to better utilize coal supplies, however, the chemical structure of coal needs to be known in much greater detail so that methods can be developed to convert coal to a clean burning liquid or gaseous fuel.

Coal is known to be a physically heterogeneous substance with inorganic mineral matter mixed randomly in the organic material. The organic matter is further subdivided into maceral groups which reflect the floristic assemblages available at the time of the formation of the coal measures. The chemical structural detail of the organic components of these materials is not well known, even though researchers have been working for decades on structure analysis. Of interest is the nature of the carbon skeleton including the aromatic and aliphatic groups; the level, type and role of oxygen, nitrogen, and sulfur; the type and extent of cross-linking; and the molecular weight distribution of the macromolecules.

Useful reviews and monographs published on coal structural analysis include works by Van Krevelan (1), Ignasiak (2), Tingey and Morrey (3), Davidson (4), Larsen (5), and Karr (6). These reports indicate the following: Coal is a highly aromatic substance (65-90% aromatic carbon, variable with rank but with few coals having aromaticities lower than 50%), with clusters of condensed rings (up to approximately four rings); the aliphatic part of the coal appears to be mostly hydroaromatic rings and short aliphatic chains connecting the aromatic clusters; the oxygen has been found in the form of phenols, quinones, ethers, and carboxylic acids, but less detail is known about the nature of the organic sulfur or nitrogen.

The study of the aromaticity of coal has included infrared spectroscopy (7) and various chemical methods (8,9), but the most promising analytical tool appears to be cross-polarization magic angle sample spinning nuclear magnetic resonance spectroscopy (CP/MAS C-13 NMR). This technique, initially developed by Pines, et al (10), has been successfully applied to coals by several workers in order to obtain aromatic-to-aliphatic ratios (11-14) (f_a). There is evidence that further structural information on coals and coal macerals can be gained from the CP/MAS C-13 NMR experiments (15-19). The aliphatic part of coal has also been characterized by a novel chemical method involving a trifluoroacetic acid/aqueous hydrogen peroxide oxidation of the aromatic rings to yield aliphatic acids and diacids (20). Chemical test results may be spurious, however, due to the severity of the reaction conditions and the insoluble and heterogeneous nature of coals.

CP/MAS ^{13}C NMR offers a powerful non-destructive tool for the analysis of carbonaceous solids. Depending on the nature of the carbonaceous material and the concomitant resolution obtainable, a wide range of structural information can be obtained. In complex organic sediments, the diversity of structural components leads to broad bands that frequently lack detail. However, employing multiple pulse techniques, it is possible to obtain additional structural information. The dipolar dephasing technique reported by Opella (26,27) discriminates protonated from nonprotonated carbons in a CP/MAS spectrum on the basis of the ^1H - ^{13}C dipolar interaction. Hagaman and Woody (28) have reported the spectra of Illinois No. 6 coal.

We wish to report data on a series of whole coals and coal macerals using conventional CP/MAS, dipolar dephasing, and 2-D dipolar dephasing techniques. These data provide a wealth of new structural information and demonstrate that multiple pulse and 2-D spectroscopic techniques can be utilized on complex carbonaceous materials. We also report data obtained on maceral samples separated by the density gradient centrifugation method which separates coal maceral groups according to density.

EXPERIMENTAL

All ^{13}C NMR CP/MAS spectra were obtained on a Bruker CXP-100 instrument equipped with a Z32DR ^{13}C -MASS superconducting magnet probehead for proton enhanced magic angle spinning experiments (CP/MAS). Samples were packed in carefully prepared rotors machined from boron nitride (body material) and Kel-F (spinner head material) in Andrew-Beams type rotors (22). Boron nitride is used as the body material because of its good tensile strength and its resistance to deformation at high spinning speeds, whereas the Kel-F material is used for the rotor head material because of its better resistance to wearing as it comes into occasional contact with the stator assembly during start ups and stops. Both materials are free of carbon and hydrogen which would cause extraneous resonance signals and decoupler heating problems. The spinning speed was slightly in excess of 4 KHz to avoid complications due to overlapping of spinning side bands with other spectral components. The carbon-proton cross polarization time was 1.5 msec and the cycle time was 0.3 seconds. Experiments performed at this laboratory have shown that such short cycle times are indeed feasible with coals because of the inherent free radical induced short relaxations times (23). Each spectra resulted from averaging 10,000 repetitions on samples of approximately 100 mg size. The dipolar dephasing experiments involved a 40 μsec delay inserted between the contact time and the acquisition period. It is well known that this delay period will decrease the signal intensities of all carbon peaks compared to their intensities in the normal CP/MAS spectrum due to T_2 relaxation effects; however, no effort has been made to correct for this decrease in intensity to effect a material balance between compared spectra since it is assumed that the decrease in intensity of the nondipolar dephased carbon-13 peak is small. Chemical shifts are reported referenced to TMS. Hexamethyl benzene was used as an external referencing material. A rotor of the reference solid is used to adjust the magic angle and the carbon/proton power levels for the Hartman Hahn condition such that the aromatic and aliphatic carbon peaks are of essentially equal intensities. The coal samples were then substituted using the same rotor without changing any resolution or referencing parameters. The upfield peak of hexamethylbenzene is presumed to be at 18 ppm from TMS.

COAL MACERALS AND MACERAL SEPARATION

The coals designated as PSOC-2 and PSOC-858 were obtained from the Coal Data Bank at the Pennsylvania State University. The maceral groups from this coal were separated by the density gradient centrifugation technique described by Dyrkacz (24,25). The samples designated by PSMC-67, -19, -34, -43, -47, and -53 were vitrinite concentrates obtained from Professor Alan Davis at Penn State and the analytical and CP/MAS data have been previously reported (16). The British maceral concentrates designated as Aldwarke, Silkstone, Teversil, Dunsil, Woolley, Wheatley Lime, Markham Main, and North Celyen were obtained from Professor Peter Given at Penn State and the analytical data on these coals are given in Table III. The samples were provided to Professor Given by the British National Coal Board and were stored under nitrogen since their preparation.

RESULTS AND DISCUSSION

We have recently established in our laboratory the capability to separate coal macerals by the density gradient centrifugation technique (DGC) described by Dyrkacz (24,25). The DGC fractogram of PSOC-2 is presented in Figure 1 indicating the density delineation of the three maceral groups. The mean densities indicated in the Figure correspond to the lipinites (largely sporinite, see Table I) vitrinite and inertinite maceral fractions. The actual density ranges for the six different samples studied are used as labels for each spectrum illustrated in Figure 2 along with the separate f_a values. This coal contains essentially no lipinites and hence exhibits only two peaks corresponding to vitrinite and inertinites (semi-fusinite and fusinite). The stacked CP/MAS spectra of the PSOC-2 whole coal and the sporinite, three vitrinite, and two inertinite fractions separated by the DGC technique are given in Figure 2. Note the variation in the band shapes in the aliphatic regions of the vitrinite and inertinite maceral groups. These data clearly indicate that additional structural information is obtainable from studies of coal maceral groups which have been separated from a given coal as previously reported (17,18). Even within the three vitrinite samples, large variations in spectral characteristics indicate structural differences among macerals of small density variance. Similar structural changes are observed in the vitrinite maceral group for PSOC-858.

Additional structural information can be obtained by means of the dipolar dephasing technique reported by Opella (26,27) which discriminates protonated from nonprotonated carbons in a CP/MAS spectrum on the basis of the ^1H - ^{13}C dipolar interaction. Hagaman and Woody (28) have reported the spectra of Illinois No. 6 coal by employing this technique. In model compounds, Alemany (29) has observed that a 40- μs interruption in the proton decoupling will cause all of the CH and CH₂ resonances to vanish, while the intensity of the nonprotonated carbons experience only minor attenuation (ca. 10-20%). The dephasing of a methyl group is more complex but approximately 50% of the methyl carbon signal is still observed after a 40 sec dephasing delay. Hence, by appropriately varying the interruption of the decoupler one can differentiate among methine/methylene, methyl and nonprotonated carbons. Typical results are given in Figure 3 for the Aldwarke Silkstone exinite. The fraction of the carbon in the sample which is aromatic and nonprotonated, f_a^{N} , is obtained by comparing the relative intensities of the aromatic region of the spectra with decoupler pulse delays of 0 and 40 sec before data acquisition. The fraction of protonated aromatic

carbon is then f_a^H ; thus $f_a^H + f_a^N = f_a$. Using a solvent refined coal tar for which high resolution 1H and ^{13}C NMR data were taken, Wilson (30) has obtained values of f_a , and f_a^H in the solid tar. These values agree nicely with those corresponding values obtained for the dissolved tar. ($f_a = 0.62, 0.62$; $f_a^H = 0.24, 0.23$ for the solid and dissolved solvent refined coal, respectively).

Dipolar dephasing data (26,17) have been acquired on 36 coal and maceral samples and some of the results are given in Table II. The data are indicative again of the highly variable structure found in coal samples. The values designated as f_s^S and f_a^B are the fraction of aromatic carbon atoms which are substituted and those which are bridgehead carbons respectively. This separation is based strictly on the chemical shift range of the nonprotonated aromatic carbons; i.e., in the dipolar dephasing spectrum, it is assumed that nonprotonated carbon resonance shifts greater than 133 ppm are substituted while those with chemical shifts less than 133 ppm are bridgeheads. This arbitrarily chosen chemical shift value has, of course, been assigned from previous experience using the spectral assignments of known compounds. The values found in the last column of Table II reflect the fraction of the aliphatic region which is both nonprotonated carbons and methyl group carbons and has been designated as f_s^* . If the carbon resonances due to these two differing types of species are distinctive, they can be further identified with the use of 2-dimensional dipolar dephasing techniques based on their differing dephasing rates. Carbon-13 data obtained on a series of British maceral concentrates are also expressed in Table II. Further analytical data for these concentrates are found in Table III. The data found in this table has been supplied by the Coal Survey National Coal Board. The Woolley Wheatly Lime sample is 93% fusinite while the Teversal Dunsil concentrate is 80% semifusinite with 13% fusinite. The Aldwarke Silkstone sample contains 43% semifusinite and 43% fusinite. The petrographic analysis of PSOC-2 reveals nearly equivalent amounts of fusinite, semifusinite, micrinite, and macrinite (6.8, 8.1, 7.5 and 8.5% respectively in the whole coal). The differences in f_a^H values for these samples are greater than the experimental error and these differences suggest that NMR techniques may be useful in characterizing the chemical structural differences between inertinite macerals.

The use of 2-D ^{13}C NMR techniques in liquids has progressed from a novelty to a very useful analytical tool. Even though the use of 2-D pulse techniques on solids is not as advanced, experiments on simple organic compounds have appeared in the literature (31). The principal value of 2-D spectroscopy in solid CP/MAS studies of coal and related macerals lies in the ability of such methods to separate spectral information which in the typical one dimensional case appears as a single resonance. Figure 3 is a 2-D contour plot of the Aldwarke Silkstone exinite maceral exhibiting chemical shift along the F_2 axis. It should be emphasized here that those carbon resonances which extend further along the F_1 axis have larger dipolar dephasing effects working upon them. Such effects can then be graphically used to differentiate between carbons of similar chemical shift but differing proton environments. Figure 5 is a stack plot of the same information found in Figure 3. Spectral traces differ from each other by 977 Hz starting with the top spectrum at zero Hz dipolar dephasing rate.

The capability of measuring directly the fraction of aromatic carbon, f_a relative to total carbon via solid ^{13}C NMR has stimulated considerable interest. The f_a values previously found (32,33) for coal macerals have been consistent with the order fusinite > micrinite > vitrinite > exinite given by Dormans et al (34) for macerals of a specific rank. For the sample set of PSOC-2 and its separated maceral groups, the f_a values found in this study are in the order inertinite > vitrinite > exinite as expected. An interesting observation is that f_a^H , the fraction of the total carbon in the coal that is aromatic and protonated, decreases in that same order for this series of six macerals. These data imply that there is a significant diversity in the amount of ring substitution and/or cross linking among the aromatic carbons in the various macerals as seen in the estimated values for the fraction of aromatic substituted and bridgehead carbons, f_a^S and f_a^B . An examination of the pure vitrinite series PSMC-67, -19, -34, -43, -47, and -53, which is a suite of samples from a common depositional environment but of varying rank, reveals a similar trend in samples of increasing rank. The CP/MAS data reported earlier (16) exhibited a decrease in functionality with progressing rank (i.e., loss of alkyl and aromatic oxygen groups). The dipolar dephasing data of this report indicate that this loss of functionality leads to a net increase in the fraction of protonated aromatic carbons. Ring condensation reactions alone cannot explain these results as ring condensation would produce an opposite effect. It appears that reactions associated with vitrinite maturation in these samples must also include some ring protonation reactions accompanying ring defunctionalization and the data suggests that these protonation reactions are preferred to ring condensation reactions.

Data on the set of British maceral concentrates, Table I, exhibit trends similar to those noted above. Comparing the f_a^H data on the inertinite fractions from PSOC-2, Woolley Wheatley Lime, Teversal Dunsil, and Aldwarke Silkstone reveals some significant differences between these samples from coals of high volatile bituminous rank (albeit, perhaps from quite different environments).

Carbon resonances arising from both nonprotonated and protonated aromatic carbons may appear at the same frequency under proton decoupling. Yet these two resonances could possess very different relaxation behavior and in a solid could evolve very differently due to local proton dipolar fields which attenuate with the carbon proton distances as $1/r_{\text{CH}}^3$. When the spin locking pulse for proton nuclei is turned off, carbons with directly bound protons such as methines and methylenes rapidly dephase in the local proton fields and their spectral response is rapidly diminished. The rapid internal motion of CH_3 groups greatly decreases the effectiveness of methyl protons. Nonprotonated carbons are only dephased by remote and therefore much weaker magnetic fields. This type of response is given in Figure 2 using the pulse sequences first proposed by Rybaczewski et al (31) and popularized by Opella (26,27) for powders. These two spectral traces demonstrate how carbon atoms with protons are significantly attenuated following a 40 μsec dephasing time. Thus, the upfield portion of the aromatic peak due to protonated carbons and essentially all of the aliphatic region are attenuated leaving primarily the nonprotonated aromatic carbons and methyl carbons (the two high field peaks in the lower trace which have chemical shift values for aliphatic and aromatic CH_3 carbons). The small vestigial remnant of the once very strong methine/methylene peak appears as the lowest field peak of the three distinct aliphatic peaks. Thus, this spectral response is limited to a subportion of the total spectrum contained in the upper trace.

Thus, otherwise overlapping spectral information has been obtained by employing in a subtle way the differing dipolar properties of the different types of carbons. If this spectral feature is made the basis of a two dimensional, 2-D, FT spectrum, one may simultaneously obtain spectral information on both nonprotonated and protonated carbons directly. Figures 3 and 4 contain such a 2-D spectrum for the Aldwarke Silkstone exinite. In Figure 4 a contour plot of the spectral intensities is given for the rate of dipolar dephasing along the y-axis vs. chemical shift along the x-axis. Thus, the nonprotonated and methyl carbons show steep fall off in the intensity contours while protonated carbons are represented by much broader (along y-axis) spectral responses. Vertical cuts through the 2-D surface along the chemical shift axis are given in Figure 5. Hence, we observe in a more typical format the spectral response as a function of a dipolar dephasing frequency. For a solid powder the C-H dipole-dipole vectors span all possible orientations and thus zero frequency responses are found for all resonances, albeit the spread in aliphatic response is distributed over such a much greater range of dephasing frequencies as to reduce this part nearly to the noise level. The successive slices in Figure 5 leaves the CH₂ peak persisting to higher dephasing frequencies as would be expected from the data in Figure 3. There is an inverse relationship between the time slices in Figure 3 and the frequency slices in Figure 5. Short times contain information corresponding to larger dephasing frequencies. The three dimensional plot (Figure 6) of the aromatic portion of Figures 4 and 5 helps one to appreciate the above point. Note in the plot sharp peaks corresponding to nonprotonated carbons. This feature is graphically shown in the 3-D portrayal. A single chemical shift slice through the aromatic region, also shown in Figure 5, emphasized the dual nature of the spectral response with a sharp peak resting on a broad base peak. Curve fitting techniques can easily resolve the true components.

Thus, using very sophisticated spectral resolving techniques, important structural information on coal is now available from these techniques for the first time. Hence, multiple pulse/multidimensional spectroscopy offers an exciting new analytical tool for the study of complex materials such as coal and coal macerals.

ACKNOWLEDGMENT

This work was supported by the Department of Energy Office of Energy Research under Contract No. DE-AS02-78ER05007 and the Office of Basic Energy Sciences, Division of Chemical Sciences, U. S. Department of Energy under Contract No. 31-109-ENG-38. We are indebted to Professor Peter Given for supplying the British maceral concentrates which were obtained from the British National Coal Board.

REFERENCES

1. P. W. Van Krevelan, "Coal" Elsevier Publishing Company, New York, 1961.
2. B. S. Ignasiak, T. M. Ignasiak, and N. Berkowitz, Reviews in Analytical Chemistry, 1975, 2, 278.
3. G. L. Tingey, and J. R. Morrey, "Coal Structure and Reactivity", TID-16627 Batelle Pacific Northwest Labs, Richland Washington, 1973.

4. R. M. Davidson, "Molecular Structure of Coal" IEA Coal Research, London, 1980.
5. J. W. Larsen, "Organic Chemistry of Coal" ACS Symposium Series 71, Washington, D.C. 1978.
6. C. Karr, "Analytical Methods for Coal and Coal Products", Vol. I-III, Academic Press, New York, 1978.
7. H. L. Retcofsky, Applied Spectroscopy, 1977, 31, 166.
8. S. K. Chakrabartty, and H. O. Kretschmer, Fuel, 1974, 53, 132.
9. J. L. Huston, et al, Fuel, 1976, 55, 281.
10. A. Pines, H. G. Gibby, and J. S. Waugh, J. Chem. Physics, 1973, 59, 569.
11. D. L. VanderHart, and H. L. Retcofsky, Fuel, 1976, 55, 202.
12. V. J. Bartuska, G. E. Maciel, J. Schaefer, and E. O. Stejskal, Fuel, 1977, 56, 354.
13. V. J. Bartuska, G. E. Maciel, and F. P. Miknis, "C-13 NMR Studies of Coals and Oil Shales," American Chemical Society, Division of Fuel Chemistry, Preprints, 1978, 23.
14. K. W. Zilm, R. J. Pugmire, D. M. Grant, W. A. Wiser, and R. E. Wood, Fuel, 1979, 58, 11.
15. K. W. Zilm, R. J. Pugmire, S. R. Larter, J. Allen, and D. M. Grant, Fuel, 1981, 60, 717.
16. R. J. Pugmire, D. M. Grant, S. R. Larter, J. Allen, A. Davis, W. Spackman, and J. Sentfle, New Approaches in Coal Chemistry, ACS Symposium Series No. 169, 1981, p 23.
17. R. J. Pugmire, K. W. Zilm, W. R. Woolfenden, D. M. Grant, G R. Dyrkacz, C. A. A. Bloomquist, and E. P. Horwitz, Proceedings of the International Conference on Coal Science, Dusseldorf, Germany, September 7-9, 1981, p. 798-806.
18. R. J. Pugmire, K. W. Zilm, W. R. Woolfenden, D. M. Grant, G. R. Dyrkacz, C. A. A. Bloomquist, and E. P. Horwitz, Carbon-13 NMR Spectra of Macerals Separated from Individual Coals, in press.
19. A. Pines and D. E. Wemmer, "Developments in Solid State NMR and Potential Applications to Fuel Research", ACS Division of Fuel Chemistry, Preprints, 1978, 23, 15.
20. N. C. Deno, B. A. Greigger, and S. G. Stroud, Fuel, 1978, 57, 455.

21. P. H. Given W. Spackman, A. Davis, and R. G. Jenkins, Coal Liquefaction Fundamentals, D. D. Whitehurst, Ed. ACS Symposium Series No. 139, Washington, D.C., 1980, p. 334.
22. K. W. Zilm, D. W. Alderman, and D. M. Grant, J. Mag. Res., 1978, 30, 563.
23. K. W. Zilm, R. J. Pugmire, and D. M. Grant, ^1H and ^{13}C Relaxation in Coals: Effects on Quantitation, manuscript in preparation.
24. G. R. Dyrkacz and E. P. Horwitz, Fuel, 1982, 61, 3.
25. G. R. Dyrkacz, C. A. A. Bloomquist and E. P. Horwitz, Sep. Sci. and Tech., 1981, 15, 1571.
26. S. J. Opella, and M. H. Fry, J. Amer. Chem. Soc., 1979, 101, 5854.
27. S. J. Opella, M. H. Fry, and T. A. Cross, J. Amer. Chem. Soc., 1979, 101, 5856.
28. E. W. Hagaman and M. C. Woody, Proceedings of the International Conference on Coal Science, Dusseldorf, September 7-9, 1981, pp 34-38.
29. L. B. Alemany, R. J. Pugmire, D. M. Grant, T. D. Alger, and K. W. Zilm, Cross Polarization and Magic Angle Spinning NMR Spectra of Model Organic Compounds III. The Effect of Dipolar Interaction on Cross Polarization and Carbon-Proton Dephasing, manuscript in preparation.
30. M. A. Wilson, R. J. Pugmire, N. J. Russell, and D. M. Grant, Structure of Australian Oil Shales and Solvent Refined Coal as Revealed by ^{13}C CP/MAS Studies, manuscript in preparation.
31. E. F. Rybaczewski, B. L. Beff, J. S. Waugh, and J. S. Sherfinski, J. Chem. Phys., 1977, 67, 1231.
32. R. E. Richards and R. W. York, J. Chem. Soc., (London), 1960, 2489.
33. H. Tschamler and E. deRuiter, Coal Science, R. F. Gould, Ed., Advances in Chemistry Series 55, American Chemical Society, Washington, D.C., 1966, p 332.
34. H. N. M. Dormans, F. J. Hutjens, and D. W. Van Krevelen, Fuel, 1957, 36, 321.

TABLE I
Elemental Analysis and Maceral Composition of Coal PSOC-2 Separated
by Density Gradient Centrifugation Techniques

Petrographic Analysis (Volume %)	COAL PSOC-2
<u>Liptinites</u>	
Alginites	0.0
Resinite	1.2
Cutinite	1.4
Sporinite	33.6
<u>Vitrinite</u>	29.6
<u>Inertinites</u>	
Micrinite	8.7
Semifusinite	8.3
Fusinite	7.0
Macrinite	7.7
Total Liptinites	36.2
Total Vitrinite	32.1
Total Inertinites	31.7
Elemental Analysis (DMMF %)*	
C	85.49
H	5.56
N	1.46
S	0.62
O (by difference)	6.79
Mineral Matter Content of Coal* (Before Demineralization)	3.82
Vitrinite Reflectance* (Mean maximum)	0.89
Class*	HVAB
Coal Type	Channel Lithotype

* Values reported by Penn State on different samples of the same coal.

TABLE II
Structural Parameters of Coals and Coal Macerals

	H/C	%C (DMMF)	f_a	f_a^H	f_a^N	f_a^B	f_a^S	f_s^H	f_s^*
PSOC-2	0.79	86.61	0.60	0.39	0.21	0.11	0.10	0.36	0.05
E	-	-	0.34	0.24	0.10	0.02	0.07	0.59	0.06
V-1	-	-	0.61	0.41	0.20	0.07	0.13	0.33	0.06
V-2	-	-	0.70	0.45	0.25	0.10	0.15	0.26	0.04
V-3	-	-	0.67	0.47	0.20	0.11	0.09	0.26	0.07
I-1	-	-	0.75	0.59	0.17	0.06	0.11	0.21	0.04
I-2	-	-	0.76	0.63	0.13	0.05	0.08	0.19	0.07
PSMC-67	0.80	82.2	0.73	0.29	0.44	0.23	0.21	0.22	0.05
-19	0.86	84.4	0.77	0.35	0.33	0.18	0.15	0.20	0.03
-34	0.75	83.9	0.77	0.42	0.35	0.19	0.16	0.20	0.03
-43	0.78	87.0	0.78	0.44	0.34	0.20	0.14	0.19	0.03
-47	0.73	88.0	0.86	0.43	0.43	0.26	0.16	0.12	0.02
-53	0.63	89.1	0.85	0.48	0.38	0.22	0.16	0.13	0.01
Aldwarke									
Silkstone									
Exinite	1.02	87.2	0.53	0.26	0.27	0.14	0.13	0.40	0.07
Vitrinite	0.75	86.9	0.80	0.38	0.42	0.21	0.21	0.15	0.05
Inertinite	0.48	92.1	0.89	0.59	0.30	0.17	0.13	0.10	0.01
Teversil									
Dunsil									
Vitrinite	0.75	81.5	0.78	0.30	0.48	0.23	0.25	0.18	0.04
Inertinite	0.53	87.7	0.86	0.37	0.49	0.21	0.28	0.12	0.02
Woolley									
Wheatley, Lime									
Exinite	0.95	87.9	0.47	0.29	0.18	0.09	0.09	0.46	0.07
Vitrinite	0.78	86.6	0.77	0.48	0.29	0.12	0.17	0.20	0.03
Inertinite	0.37	93.7	0.89	0.53	0.36	0.21	0.15	0.09	0.02
Markham Main									
Exinite	1.08	82.6	0.45	0.25	0.20	0.09	0.12	0.48	0.07
Vitrinite	0.80	82.2	0.76	0.33	0.41	0.23	0.18	0.21	0.06
Inertinite	0.47	91.6	0.82	0.51	0.31	0.18	0.13	0.15	0.03
North Celyen									
Exinite	0.65	90.6	0.84	0.40	0.44	0.27	0.17	0.14	0.02
Vitrinite	0.67	89.9	0.83	0.46	0.37	0.24	0.13	0.16	0.01
Inertinite	0.61	91.3	0.85	0.47	0.38	0.24	0.14	0.14	0.01
PSOC-1108	0.65	68.0	0.43	0.29	0.14	0.06	0.08	0.46	0.11
PSOC-1110	0.93	72.5	0.16	0.03	0.13	0.06	0.07	0.65	0.19
Beluga									
Lignite	0.94	65.7	0.64	0.17	0.47	0.07	0.40	0.25	0.11

$$f_a = f_a^H + f_a^N = f_a^H + f_a^S + f_a^B \quad f_s = f_s^H + f_s^*$$

$$f_a + f_s = 1$$

f_s^* = Non-protonated aliphatic carbon plus methyl carbons.

Table III. Analytical Data for British Maceral Concentrates

Colliery Seam	Woolley			Markham Main			Teversal			Aldwarke			North Celynen		
	V	E	I	V	E	I	V	E	I	V	E	I	V	E	I
H ₂ O, as anal., %	1.6	0.7	0.5	6.9	2.0	1.8	9.2	-	4.1	1.7	0.7	0.8	1.0	0.6	0.7
VM dmwf	36.1	57.8	9.0	40.1	73.7	18.1	35.1	-	21.5	33.2	66.5	15.4	24.4	22.2	19.4
C dmwf	86.6	87.9	93.7	82.2	82.6	91.6	81.5	-	87.7	86.9	87.2	92.1	89.9	90.6	91.3
H	5.6	6.9	2.9	5.5	7.4	3.6	5.1	-	3.9	5.4	7.4	3.7	5.0	4.9	4.6
N	1.8	1.1	0.4	1.9	1.1	0.4	2.0	-	1.1	1.8	1.2	0.7	1.6	1.4	1.2
S	1.1	1.1	0.2	1.1	1.6	(0.3)	0.6	-	0.4	0.73	0.6	0.4	0.68	(0.6)	(0.5)
O (diff.)	4.9	3.0	2.8	9.3	7.3	4.1	10.8	-	6.9	5.17	3.6	3.1	2.82	2.5	2.4
Rank	HVA	-	-	HVB	-	-	HVB	-	-	HVA	-	-	MVB	-	-
MM	1.4	2.8	4.9	1.4	0.9	6.0	0.4	-	2.9	0.8	0.3	5.0	2.9	4.5	8.87*
Vitrinite	96.0	10.0	4.0	98.0	3.0	6.0	98.0	-	6.0	98.0	0.0	4.0	86.0	40.0	15.0
Exinite	3.0	79.0	tr	tr	88.0	1.0	1.0	-	tr	1.0	95.0	-	3.0	30.0	11.0
Inertinite	1.0	11.0	96.0	2.0	9.0	92.0**	1.0	-	93.0*	1.0	5.0	96.0	11.0	30.0	71.0

* semifusinite

** equal amounts fusinite and semifusinite

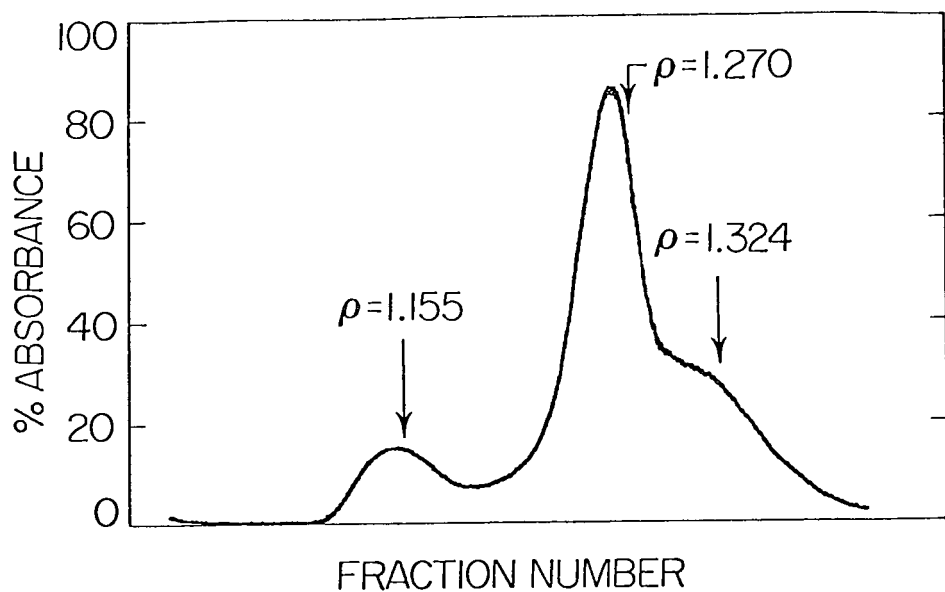


Figure 1. Fractogram for analytical DGC separation run on PSOC-2. The densities indicate the separation of the liptinite, vitrinite, and inertinite maceral groups.

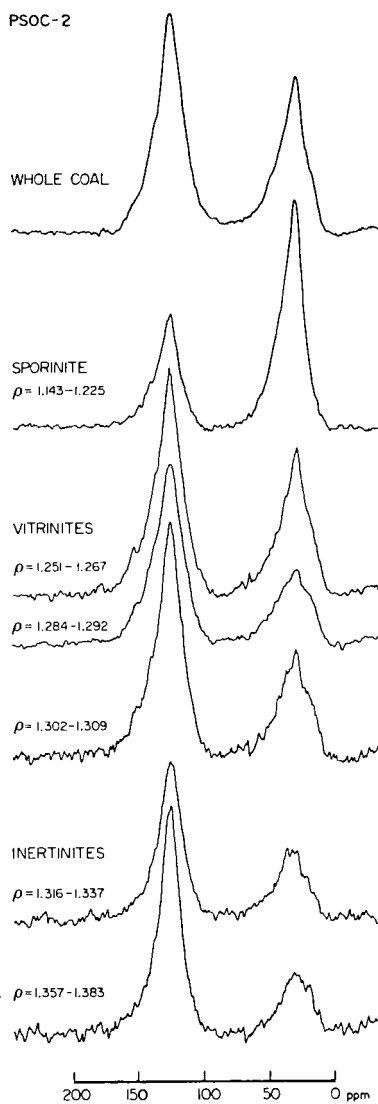


Figure 2. CP/MAS spectra of PSOC-2 whole coal and the maceral groups separated from the coal by density gradient centrifugation. The density ranges represent the range of densities for samples employed. f_a values are given for each sample.

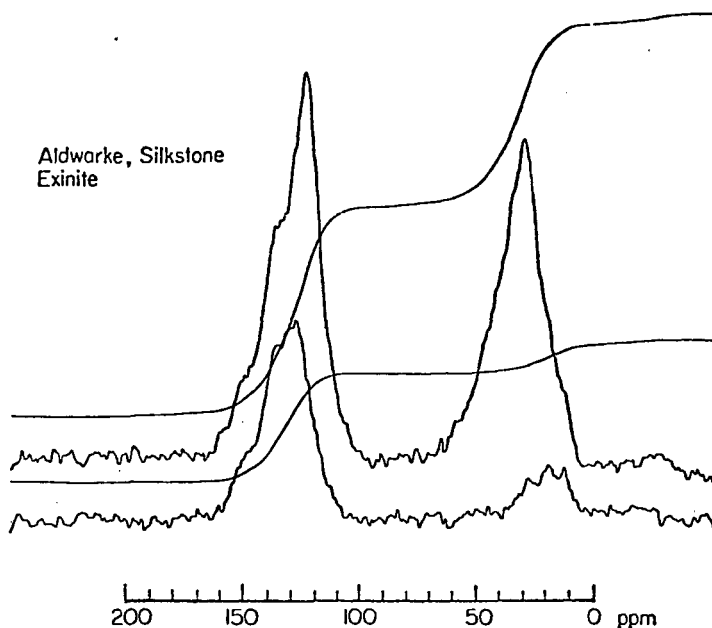


Figure 3. CP/MAS (top) and dipolar dephasing data with lower trace acquired following 40 μ sec. pulse delay. Note three separate peaks in the aliphatic region due to methyls and CH_2 's. PVC₈₂ 18

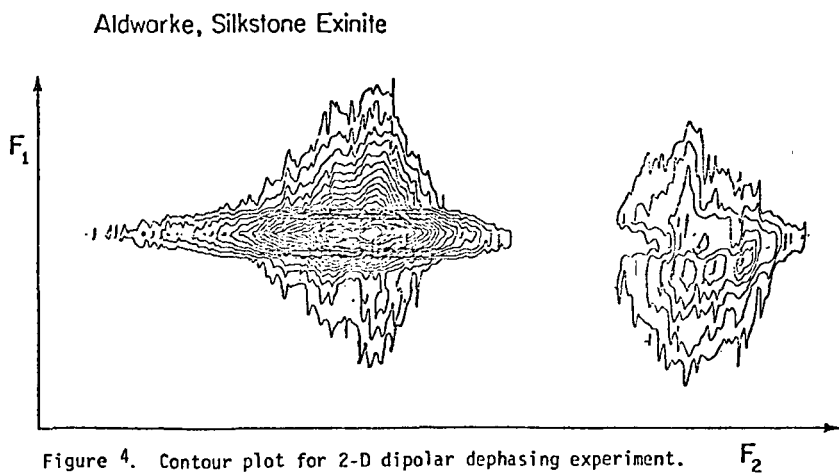
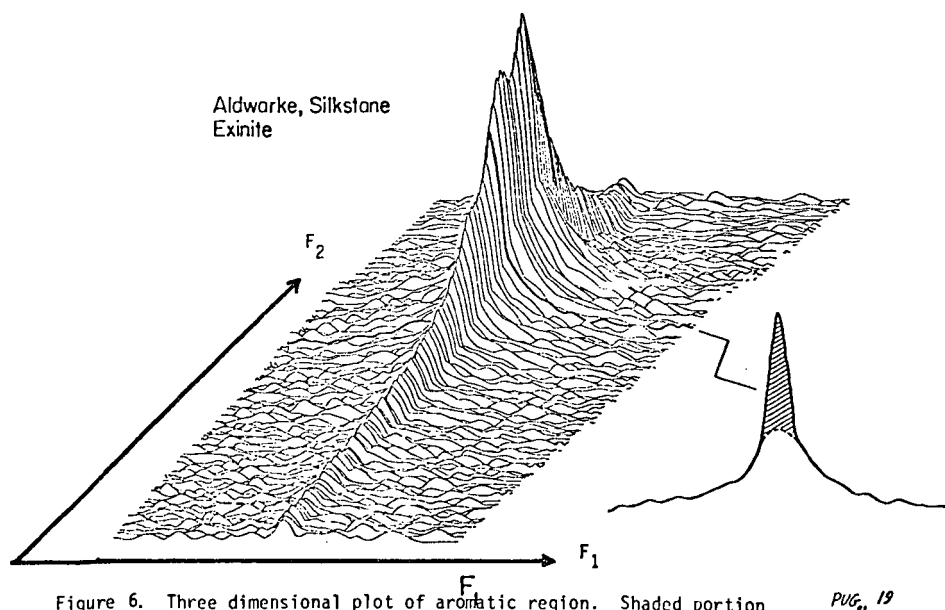
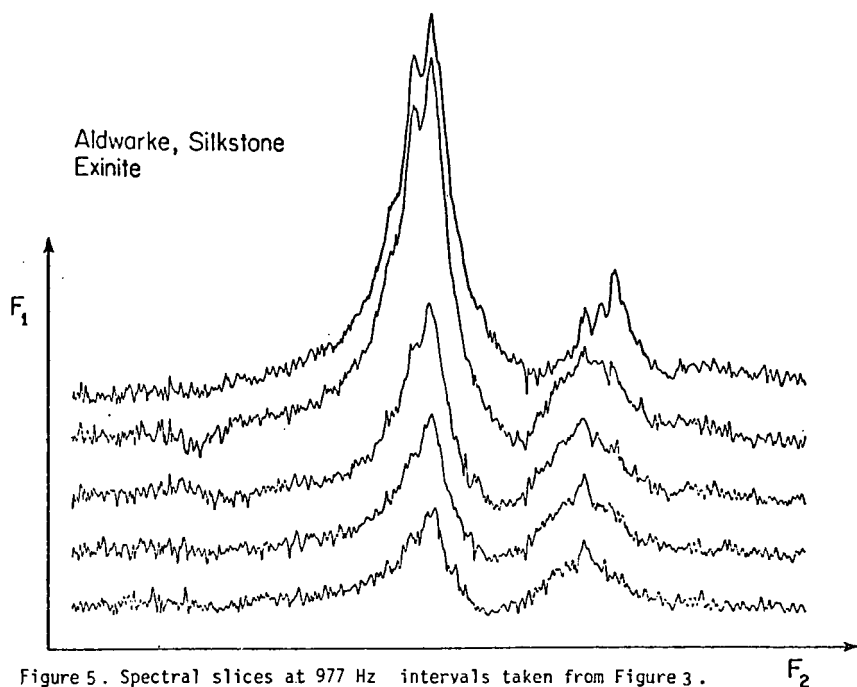


Figure 4. Contour plot for 2-D dipolar dephasing experiment.



PUG₁₉

ELECTRON SPIN RESONANCE OF ISOLATED COAL MACERALS: A PRELIMINARY SURVEY

B. G. Silbernagel and L. A. Gebhard
Corporate Research - Science Laboratories
Exxon Research and Engineering Company
Linden, New Jersey 07036

G. R. Dyrkacz
Chemistry Division - Argonne National Laboratory
Argonne, Illinois 60439

INTRODUCTION

While there have been a large number of electron spin resonance (ESR) studies of coal and coal products,⁽¹⁾ previous interpretations were based on the "average" properties of coals due to the chemical heterogeneity of the coal samples examined. The recent evolution of maceral separation techniques permits detailed ESR observations on coals of different rank, for which maceral type, and maceral density can be discriminated simultaneously. The present ESR survey of carbon radicals in separated macerals shows that each maceral type exhibits characteristic carbon radical properties. Furthermore, the properties of carbon radicals change within a given maceral type as the density varies.

EXPERIMENTAL PROCEDURES

A total of 37 samples from 16 coals of the Pennsylvania State University coal data base (PSOC) were examined. Separate fractions were obtained by isopycnic density gradient centrifugation of small ($\sim 3\mu$ m) coal particles in a aqueous CsCl density gradient.⁽²⁾ The individual samples are listed by PSOC numbers, maceral type, and density, in Table 1. After separation, the samples were kept under dry nitrogen until they were transferred to ESR tubes and sealed under helium gas. Typical ESR sample weights were approximately 10 mg. The ESR observations were conducted at 9.5 GHz in a Varian E-line ESR spectrometer with variable temperature capabilities from 90K-300K. The g-value, linewidth (defined as the splitting between peaks of the derivative curve of the ESR absorption - ΔH_{pp}) and the intensity of the carbon radical signal were observed in each case.

Before discussing the correlation of these properties, it is useful to note a significant difference in the response of carbon radicals in different maceral types to the applied microwave field. At sufficiently low microwave powers, the radical intensity varies linearly with microwave field strength, or equivalently varies as the square root of the microwave power. At higher powers, this response is less than linear, a phenomenon known as saturation, when the microwave power absorbed by the carbon radicals exceeds the radicals' ability to dissipate it to their environment. This process is illustrated in Figure 1, where the radical intensity, divided by the square root of the microwave power, is plotted as a function of the logarithm of the microwave power. The flat response at low power indicates the linear behavior; the fall-off at higher microwave

powers indicates the onset of saturation. It is clear from Figure 1 that vitrinite saturates at low powers, a fall-off being noted already at $\sim 10 \mu$ Watts of microwave power. A similar departure from linear behavior does not occur in inertinite until powers of $\sim 10^4 \mu$ W are applied. Exinite is intermediate in behavior. To avoid saturation-related problems, all samples were run at microwave powers of 3μ W, indicated by the arrow and dashed-line in the figure.

EXPERIMENTAL RESULTS

Examination of the ESR linewidth and the maceral density show clear distinctions between different maceral types. Figure 2 shows that exinite macerals have low densities and a narrow range of ESR linewidths, $\Delta H_{pp} \sim 6.5$ G. While vitrinite and inertinite show considerable overlap in maceral densities, the inertinite linewidths are dramatically smaller, $\sim 1-2$ G, as opposed to $\sim 5.5-7.5$ G for the vitrinites. This significant linewidth difference may assist in the discrimination of maceral types. As Figure 2 indicates, two macerals which petrographic analyses indicated to be inertinite, fall into the vitrinite maceral field. Since the small particle size required for separation ($\sim 3 \mu$ m) complicates the petrographic analysis, combined ESR and petrographic examinations may prove useful in future maceral type determinations. It is also interesting to note a weak trend in the vitrinite of decreasing ΔH_{pp} with increasing maceral density. Such a decrease might be anticipated if the increased maceral density resulted from a larger fraction of aromatic species, reducing proton broadening of the carbon radical linewidth.

The relationship between ESR intensity and maceral density is far less obvious, as Figure 3 indicates. Exinite samples have relatively low densities and radical intensities, as might be anticipated for aliphatic-rich macerals. Vitrinite and inertinites exhibit intensity variations in excess of an order-of-magnitude, and there is no clear variation of intensity with the physical density of the macerals. This suggests that a variety of factors, including the nature of the organic species and the details of the coalification process may serve as determinants of the number of carbon radicals.

A direct comparison of ESR linewidth and intensity, shown on Figure 4, shows a significant dependence on the type of coal sample being examined. In this case, open-circle symbols designate PSOC 106 samples, open-squares - PSOC 297, and open-triangles PSOC 1005. Solid-circles designate the balance of the vitrinite samples examined. No obvious clustering of vitrinite samples of a single type is observed. The fact that ΔH_{pp} is nearly independent of ESR intensity suggests that unresolved hyperfine interactions with adjacent protons, rather than dipole interactions between carbon radicals, are responsible for the observed linewidth.

The ESR linewidth variation with density for vitrinite macerals of different coals is presented in Figure 5. The open-symbols designate the three PSOC coals mentioned in Figure 4. As suggested in Figure 1, there is a general tendency for linewidth to decrease with increasing density. For PSOC 106 and 297, there is little density or linewidth variation observed for the vitrinites from each coal. Conversely, PSOC 1005 shows a broad range of density variations, and the linewidth increases. The source of this different behavior is still under investigation.

The isolated inertinite macerals provide an opportunity to examine their distinctly different properties. While strikingly narrower than the exinite and vitrinite ESR signals, the ESR absorption is still symmetric. The linewidth varies dramatically, from $H_{pp} = 0.89 - 2.00$ Gauss, and the linewidth is temperature independent. The intensity of the resonance absorption varies approximately as I/T , the Curie-like susceptibility expected for simple magnetic spins. Motion of these radical species could account for the relatively narrow linewidth.

CONCLUSION

We have successfully examined a suite of very small (~ 10 mg) samples by ESR. Different maceral types have strikingly different saturation behavior and are readily distinguished in a H_{pp} /density analysis. Radical intensities vary widely and are not related to physical density. Surveys of vitrinites from three of the PSOC coals suggest that intensities are reasonably similar within a given coal, but can vary significantly from one coal to the next.

At present, we are correlating these results with microanalysis of elemental composition and solid state ^{13}C NMR estimates of carbon aromaticities. These studies will be reported elsewhere.

ACKNOWLEDGMENT

We wish to express our gratitude to M. L. Gorbaty for his encouragement of this research activity and helpful comments.

REFERENCES

1. H. L. Retcofsky, "Magnetic Resonance Studies of Coal" in Coal Science and Technology, Vol. I, M. L. Gorbaty, J. W. Larsen and I. Wender, eds. (New York, Academic Press, 1982), pp. 43-82.
2. G. R. Dyrkacz and E. P. Horwitz, Fuel 61, 3 (1982).

TABLE I: MACERAL RESUME
(Indicated numbers are the maceral densities in gm/cm³)

<u>PSOC #/Maceral Type</u>	<u>Vitrinite</u>	<u>Exinite</u>	<u>Inextinite</u>
1	1.257	-	-
81	WHOLE COAL	-	-
106	1.291	1.191	1.413
	1.330	-	1.447
	1.334	-	1.475
	1.371		
151	1.385		
236	1.278		
240	1.407		
268	1.272		
285	1.276		
297	1.264	1.040	1.384
	1.271	1.149	1.436
	1.305	1.165	
	1.340	1.200	
		1.207	
317	1.317		
409	1.302		
592	1.306		
594	1.332		
852	1.314		
975	1.408		
1005	1.345		
	1.382		
	1.420		
	1.455		
	1.486		

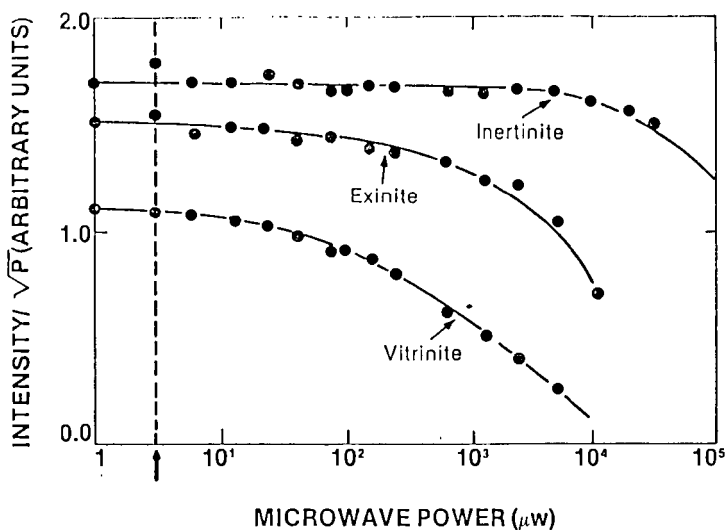


FIGURE 1: The various maceral types exhibit distinctly different microwave saturation properties.

FIGURE 2:

ESR linewidth, maceral density plots discriminate maceral types:

- ▲ = Exinite
- = Vitrinite
- = Inertinite

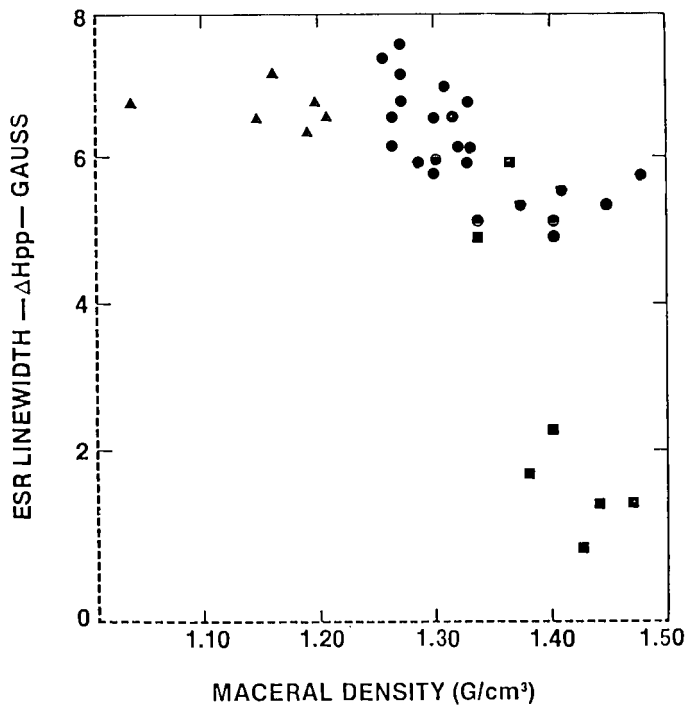


FIGURE 3: Carbon radical intensities do not depend explicitly on maceral type or maceral density.

- ▲ = Exinite
- = Vitrinite
- = Inertinite

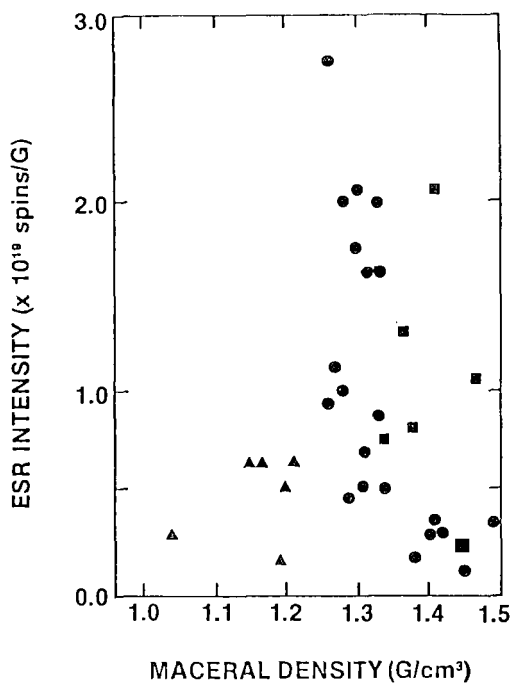
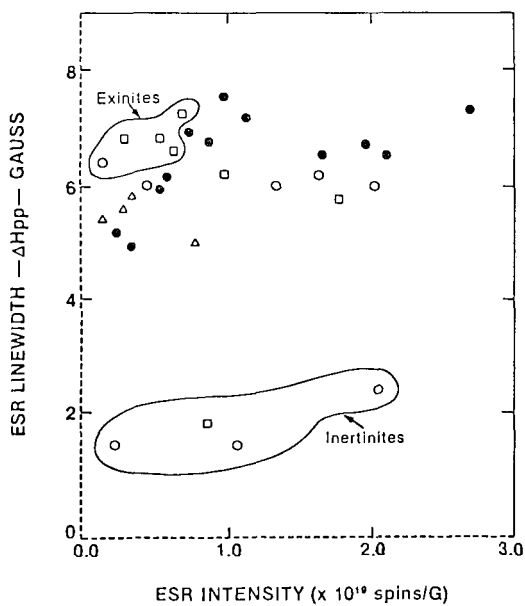


FIGURE 4: A weak variation of ESR linewidth on ESR radical intensity is observed.

- = PSOC 106
- = PSOC 297
- △ = PSOC 1005
- = All other Vitrinites



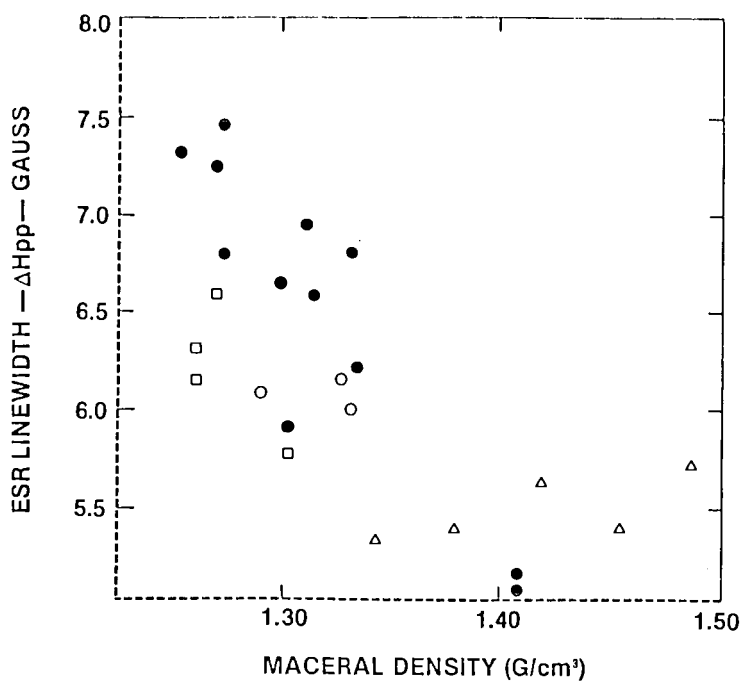


FIGURE 5: A weak decrease in ESR linewidth with maceral density is observed for vitrinite macerals. Little systematic change is observed for macerals from a given coal.

○ = PSOC 106

□ = PSOC 297

△ = PSOC 1005

● = All Other Vitrinites

PREMACERAL CONTENTS OF PEATS CORRELATED WITH "PROXIMATE AND ULTIMATE ANALYSES"

A. D. Cohen* and M. J. Andrejko

Department of Geology
University of South Carolina, Columbia, South Carolina 29208
*(presently at Los Alamos National Laboratory
Earth and Space Sciences Division, MS K586
Los Alamos, New Mexico 87545)

I. Introduction

In a number of publications, peat types have been defined petrographically by their botanical and "premaceral" compositions (1, 2, 3, 4). "Premacerals" are the organic components in the peats which, due to their color, opacity, shape, and fluorescence, can be projected as the probable progenitors of particular corresponding macerals in coals. Although the petrographic characterization of peats constitutes an important "first step" in understanding the origin and in predicting the general composition of the resultant coals, it is important that premaceral types and amounts in peats be correlated with various coal-quality tests (such as "proximate" and "ultimate" analyses). With these results it then becomes possible to develop a series of models with which to predict more precisely the chemical and physical composition of the resulting theoretical coals. These predictive characterizations can be applied not only to the projected seam-wide variability in coal quality for coals produced in similar depositional settings as that of the studied peats, but also to the prediction of the variations in industrial properties of the peats themselves, such as for gasification, liquifaction, soil conditioning, organic chemical production and so forth.

It is for these reasons that we have initiated this correlative study of peat petrography and peat industrial-chemical (coal quality) properties. Note that the information reported herein represents preliminary results based on a limited number of different types of peats that were analyzed for only a few "coal quality tests" (i.e., proximate analysis, ultimate analysis, and BTU content). Future studies will involve measurement of other petrographic parameters and include other industrial analyses (such as, gas and liquid yields, physical properties, organic chemical yields, and so forth).

II. Objectives

The objectives of this study are to:

- A. Determine the variations in premaceral types and proportions within a wide variety of peat types.
- B. Correlate premaceral contents with corresponding proximate (fixed carbon, moisture, ash, volatile matter), ultimate (C, H, O, N, S) and heating value (BTU) analyses.
- C. Predict the probable variations in the proximate and ultimate makeup and BTU levels for coals which formed in similar vegetational and depositional settings to those of the peats studied in this project.

III. Methods

Carefully extracted samples of peat were slowly dehydrated in a series of alcohol solutions and then embedded in paraffin. After embedding, thin-sections (15 microns in thickness) were cut from these samples with a sliding microtome and mounted in Canada Balsam. Details of the procedure for the embedding and sectioning of peats have previously been described by Cohen.(2,3).

Premaceral identification was made in transmitted white light, in polarized light (birefringence) and fluorescent light. Premaceral proportions were determined by area point-counting at 200 X. Proximate and ultimate analyses and BTU were obtained from commercial testing laboratories and also from the Department of Energy's Energy Technology Center at Grand Forks, North Dakota.

IV. Results and Discussion

A. Botanical Composition

Figure 1a shows the relative abundances of plant groups observed in microtome sections of the peats. Note that these peats varied considerably in their botanical compositions. The Minnesota peat consisted predominantly of Sphagnum (peat moss) debris with some grasses and conifers. The Maine peat was composed mostly of algal material with some Sphagnum and Nymphaea (water lily) debris. The North Carolina peat was dominated by bay tree (Magnolia, Persea, Gordonia) and gum tree (Nyssa) debris; while the Georgia Nymphaea peat consisted predominantly of Nymphaea debris.

Figure 1b shows the abundance of plant organs comprising the peat. Again the differences between peat types are pronounced. The Minnesota peat is dominated by roots but with lesser but equal amounts of stem and leaf debris. On the other hand, the Maine peat has the highest concentration of leaves; the North Carolina peat has the highest wood content (stems) and lowest leaf content, while the Georgia (Nymphaea) peat has the highest proportion of roots.

B. Premaceral Types and Proportions

One simplified but useful means of displaying petrographic composition of peats in thin section is by graphing the area percentages of ingredients of different colors. Figure 2 shows such a point-count for four representative types of peat from this study. Note that the Minnesota Sphagnum and Georgia Nymphaea peats have approximately the same range of colors (peaking between light-yellow and light-brown) but that the Maine peat peaked in the clear to light-yellow range while that of the North Carolina peat had peaks in the light-yellow to red-brown range and also in the dark-brown and black categories.

The Georgia Nymphaea and Minnesota Sphagnum peats tended to have the highest previtrinites while the North Carolina and Georgia Taxodium peat (not shown) had the highest prephlobaphenites (and pre-copocollinites) and also the highest preinertinites (premicrinites, prefusinites, and presclerotinites).

Figures 3 and 4 give the area percentages of birefringent premacerals found in the samples studied. Since birefringence has been equated with cellulose content, it might therefore be expected that birefringence would decrease with depth in a deposit as a result of cellulose decomposition. However, as can be seen in Figure 3 (representing two cores from the Okefenokee Swamp of Georgia), birefringence may increase or decrease with depth depending on successions of peat types and moisture conditions during initial deposition. Figure 4 shows that Georgia Nymphaea and Minnesota Sphagnum peats have the highest proportions of birefringent constituents.

The concentration of fluorescent premacerals tended to correlate slightly with the proportion of birefringent premacerals. However, different plant types were found to produce different fluorescent colors and intensities. Furthermore, natural "staining" (i.e., darkening or coloring by natural impregnation or chemical alteration) of cell walls tended to effect birefringence and fluorescence in very different ways. Natural staining tended to correlate strongly with birefringence (i.e., the darker the staining the less the birefringence), but did not correlate well with overall fluorescence properties. For example, some tissues that were highly stained tended to have higher fluorescence intensities than those that were unstained.

C. Proximate and Ultimate Analyses and BTU

Figure 5 shows the results of proximate and ultimate analyses and BTU measurement. Note that the peat from North Carolina (a lower-coastal-plain, woody, dark, more inertinite-rich sample) had the highest fixed carbon, elemental carbon and sulfur content. Woody Taxodium peats from Georgia (not shown) and South Carolina (not shown)

were similar in character to the North Carolina samples. The Georgia *Nymphaea* peats, which had the highest previtrinites, can be seen to have the highest oxygen, hydrogen, and volatile matter contents. Note that BTU values tended to correlate more strongly with ash contents than with maceral contents.

V. Summary and Conclusions

Preliminary correlations of petrographic characteristics of peats (i.e., peat types, premaceral proportions, and premaceral types) with proximate and ultimate analyses suggest the following trends:

- A. Peats with the highest proportions of birefringent macerals tend to have the highest volatile matter (and H and O contents).
- B. Fluorescence of macerals, on the other hand, seems to correlate only slightly with proximate and ultimate analyses.
- C. Higher previtrinite contents tend to correlate with higher volatile matter contents.
- D. Peats with higher preinertinites, prephlobaphenites (and pre-corpocollinites), and presclerotinites have the highest fixed carbon.
- E. BTU correlates strongly with ash content and only slightly with maceral content.

VI. Acknowledgments

This work was funded in part by Grant #EAR-79-26382 from the National Science Foundation and in part by funding from the Office of Basic Energy Sciences of the Department of Energy.

References

1. Cohen, A. D. (1968). The Petrology of Some Peats of Southern Florida (with Special Reference to the Origin of Coal), Ph.D. Thesis: Penn. State Univ., 352 p.
2. Cohen, A. D., and Spackman, W. (1972). Methods in Peat Petrology and Their Application to Reconstruction of paleoenvironments: Geol. Soc. Amer. Bull., v. 83, 129-142.
3. Cohen, A. D. (in press). Obtaining More Precise Descriptions of Peats by Use of Oriented Microtome Sections, In Proceedings of ASTM Symposium for Testing of Peats and Organic Soils. Toronto, Canada. ASTM, Philadelphia, PA.
4. Corvinus, D. A., and Cohen, A. D. (in press). Petrographic Characteristics of Carbonaceous Sediments from the Snuggedy Swamp of South Carolina. Compt. Rendu. IX Inter. Carb. Cong.

COLOR OF ALL INGREDIENTS
(AVE. OF 3 SAMPLES FROM EACH AREA)

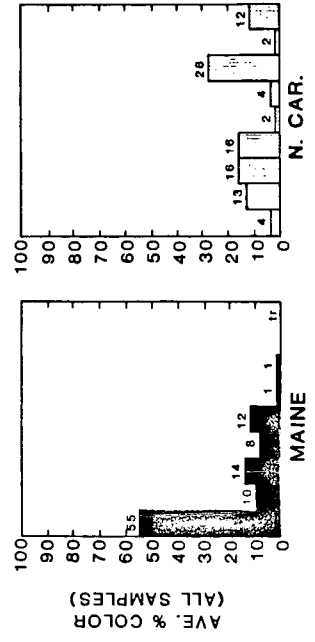
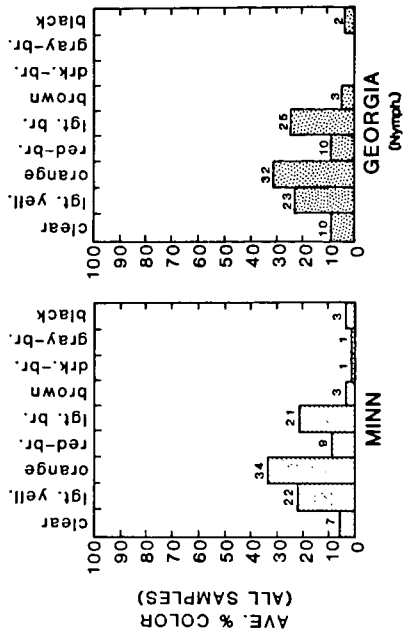


FIGURE 2

ABUNDANCE OF PLANT TYPES

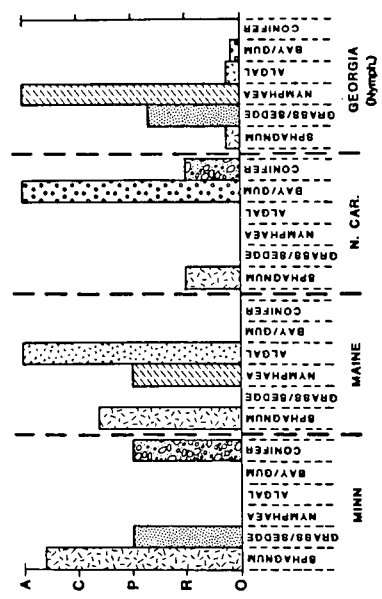


FIGURE 1a

ABUNDANCE OF PLANT ORGANS

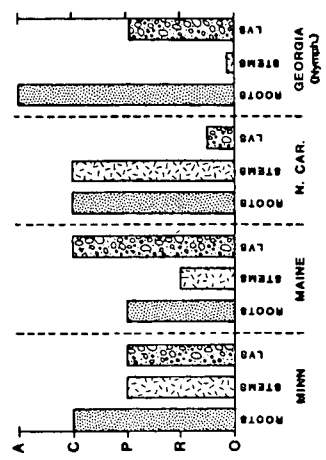


FIGURE 1b

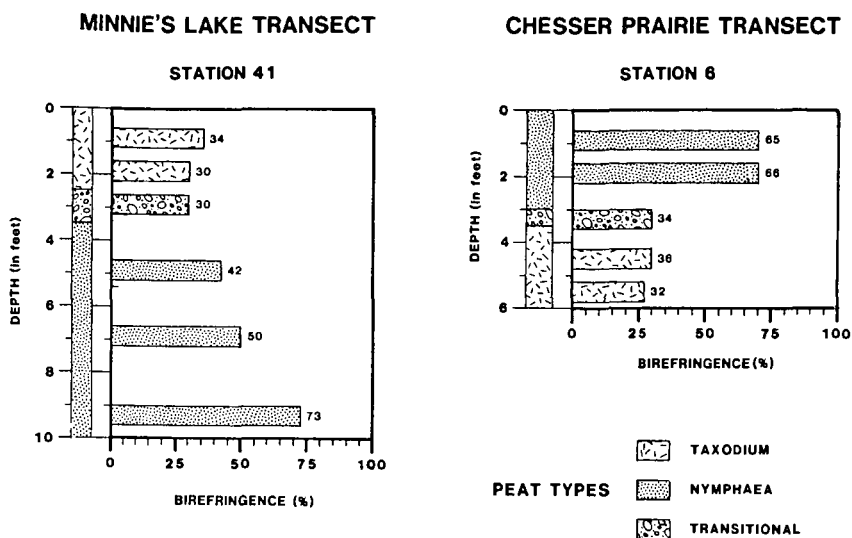


FIGURE 3

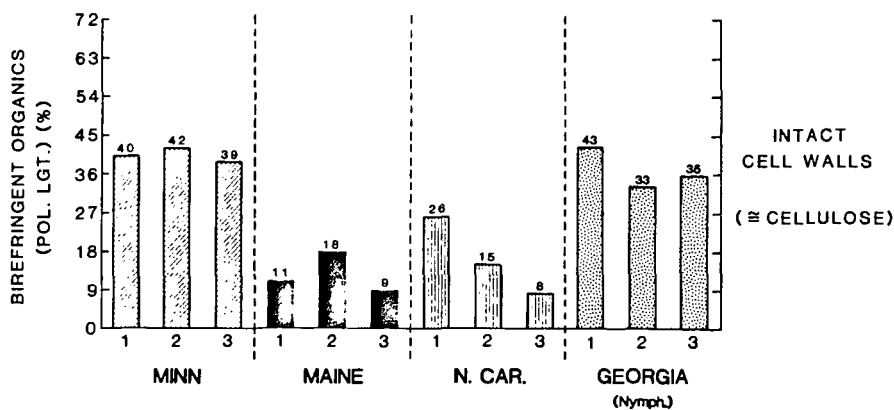


FIGURE 4

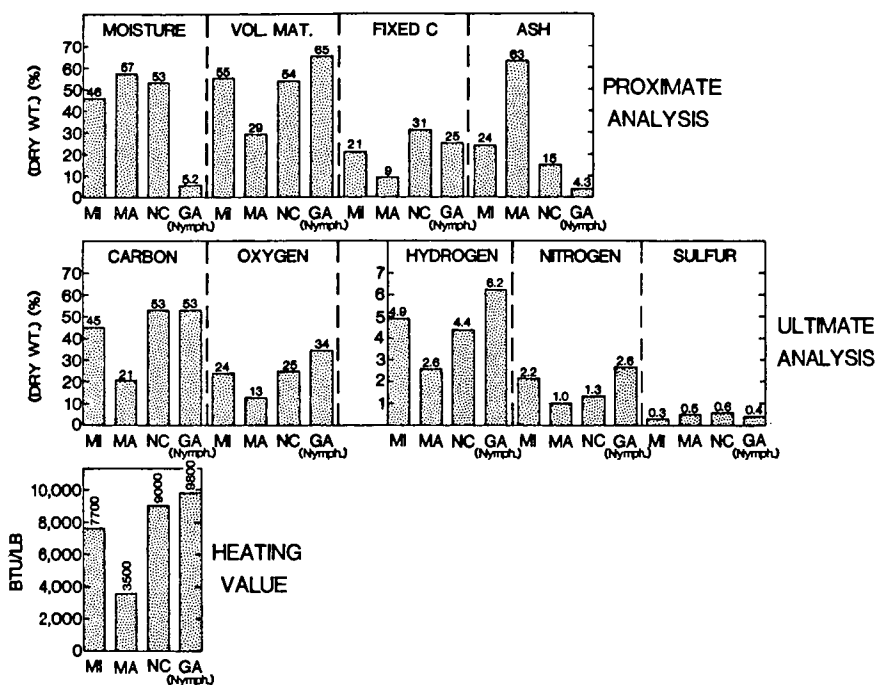


FIGURE 5

Reactivity and Characterization of Coal Macerals

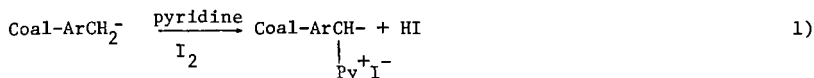
Randall E. Winans, Ryoichi Hayatsu, Robert G. Scott, and Robert L. McBeth

Chemistry Division
Argonne National Laboratory
Argonne, IL 60439

In a study of the organic structures in coals and their reactivity in chemical and thermal processes, it is desirable to reduce the complexity of the material with some sort of physical separation. One such approach is the separation of the coals into their maceral groups, which are the microscopically identifiable organic portions of coal which have different origins, chemical and physical features, and reactivity. Two bituminous coals have been separated into their three main maceral groups: exinite, vitrinite, and inertinite, using a modified float-sink technique which uses analytical density gradient centrifugation (DGC) to determine the appropriate density ranges. The DGC technique which exploits the differences in densities has just recently been reported (1,2).

The chemistry of macerals separated by DGC, float-sink and hand picking has been investigated recently by several techniques including: solid ^{13}C nmr (3,4), oxidation (5,6), and mass spectrometry (5,6,7,8). Early work focused on chemical properties (9) and esr spectroscopy (10). In the approach taken in this study the maceral concentrates were pyrolyzed in a vacuum and the resulting products collected and then characterized by gas chromatography mass spectrometry and by GC microwave plasma emission spectroscopy. The vacuum technique was chosen over the typical on-line pyrolysis-GCMS method for two reasons. First, experiments in this laboratory have shown that with the vacuum technique, secondary reactions such as aromatization of alicyclics is less likely to occur. Second, better quantitative data can be obtained with a batch type reaction scheme.

In addition to characterization of thermal products, the chemical reactivity of these concentrates has been studied. Reactive hydrogens such as benzylic types have been determined from the reaction of the macerals with pyridine and iodine to form pyridinium iodides:



It has been shown that the number of pyridinium iodides per 100 carbon atoms in the original coal decreases with increasing rank (11). Further studies have shown that these derivatized coals are activated toward oxidative solubilization using a reagent, alkaline silver oxide, which normally is quite ineffective in dissolving raw coals. In the results from the thermal and chemical reactions, similarities and differences have been noted which will be discussed later. Also, it should be emphasized that in this study we are examining maceral concentrates from the three main groups which are derived from the same coal. These coals were chosen to be representative of bituminous coals and not to be sapropelic coals where the chemistry may be more unusual due to the typically large exinite content.

EXPERIMENTAL

Two of the coals used in this study were obtained from the Penn State Coal Sample Bank. They were an HVA bituminous coal (PSOC 1103) from the Upper Elkhorn #3 seam in Eastern Kentucky and an HVA bituminous coal (PSOC 828) from the Brazil Block seam in Indiana. A third coal from which vitrinite and fusinite were hand picked was an Illinois No. 2 seam HVC bituminous coal from Northern Illinois. All

of the elemental analyses, petrographic analyses, and yields of the samples are presented in Table 1. The details of the sink-float technique have been reported previously (1). Typically, 3 micron particle size demineralized coal is centrifuged in aqueous CsCl₂ solution of the appropriate density with a small amount of surfactant added to disperse the coal particles. The exinites in the float are collected and the sink fraction is further separated into vitrinite and inertinite fractions by repeating the procedure at a higher density. The process yielded gram quantities of concentrates. The density cutoff points were determined from analytical DGC of coals of similar origin and rank. The technique used for petrographic analysis has also been reported earlier (2).

In the pyrolysis experiment, typically 30 mg of sample was heated in a quartz tube at 400°C for 24 hrs at 2×10^{-3} torr. Tars were trapped at room temperature and the more volatile products at liquid nitrogen temperature. These two fractions were analyzed by GCMPEs (MPD-850) using a 25m x 0.25 mm i.d. OV-101 fused silica column and by GCMS (Kratos MS25) using a 30m x 0.25 mm i.d. DB-5 column.

The pyridinium iodide coals were prepared by refluxing 1 g of coal or maceral concentrate in 60 ml of pyridine with 4 g of iodine for 70 hrs. The reaction mixture was poured into 10% aqueous NaHSO₃ and the solution filtered. The derivatized coal was washed free of pyridine, dried, and analyzed. Portions of the activated coal were oxidized with freshly prepared silver oxide in refluxing aqueous NaOH. The oxidation products, which were soluble in alkaline solution, were acidified and then extracted with a series of organic solvents. The major products were only soluble in alkaline solution or polar solvents.

RESULTS AND DISCUSSION

Of particular interest in this study is the nature of the non-aromatic structures, in the three main maceral groups. It should be noted that the exinites in both these coals are 90% sporinite. It has been theorized that small molecules, especially the aliphatics, are fairly mobile at some period during the formation of coal (5,6). The studies which support this theory were done on coals that were very rich in exinites and some contained alginite. The two coals chosen in the present work have a more normal distribution of macerals and yet the pyrolysis results indicate that migration of molecules from the exinites to vitrinite and then incorporation into the macromolecular structure might have occurred.

Chromatograms from the GCMPEs carbon channel of the tars from two exinites and a vitrinite are shown in Figure 1. Long chain normal alkenes and alkanes dominate the compounds in the tar along with a series of triterpenes which are slightly altered hopanes. A general structure for hopane is shown in the upper right of the figure. Several points should be made concerning these results. First, we believe that these compounds were derived from the macromolecular structures in these macerals. During the preparation of the concentrates most of the soluble molecules are removed. Evidence for this is found from examination of the extracts of the whole, untreated coals. One of the major compounds isolated is the biomarker pristane which has been identified many times previously in extracts (11) and coal liquids (12). However, this compound is absent from the pyrolysis products, although it is stable under the conditions used. At least a portion of the macromolecular structures in the exinite and vitrinite could be similar. As one would expect, the yields of these aliphatic and alicyclic compounds are less in the vitrinites. The yields follow inversely the fraction of aromatic carbons (4) in these three maceral groups. The exinite concentrate for the Kentucky coal is quite impure (50% vitrinite) which is reflected in the pyrolysis yields.

Another similarity between vitrinite and the exinite is the existence of 5 member ring triterpenes in the pyrolysates. These compounds, which show the base peak at $m/z = 191$ in their mass spectra, have been found in pyrolysis MS of alginite

(5), coal extracts (6,13), and oil shales (14) and are usually associated with some type of algal origins. It is surprising that they were found in these coals and probably more importantly, that they were not aromatized. From the GCMS it appears that only one of these peaks may represent a species containing one aromatized ring. Again these results suggest that there could have been a significant amount of molecular mobility during the early stages of the formation of this coal.

There is a much larger variation between pyrolysis product volatile fractions for the exinites and vitrinites. The sporinite yielded mostly normal alkanes and alkenes up to approximately C19 with C16 being the most abundant product. The very low molecular weight hydrocarbons such as methane and ethane were not analyzed. Also, benzene and phenol derivatives were found as minor products. The vitrinite products were dominated by aromatics such as alkylbenzenes, alkyl naphthalenes, phenols, and naphthols. The smaller alkane/alkenes were also found. These results are more consistent with what was found in pyrolysis MS of sporinites and vitrinites (5,7).

Pyrolysis results for the inertinite concentrates are fairly inconclusive due to the high concentration of vitrinite except for the I11 #2 fusinite which was quite unreactive. Pyrolysis MS of this fusinite shows mostly alkylated naphthalenes and phenanthrenes. What may be interesting is the Kentucky inertinite fraction which is thought to contain ~50% pseudo-vitrinite. This maceral which is usually categorized with vitrinites was placed in the inertinite column due to its low reactivity both in pyrolysis and in the pyridine-iodine reaction.

In the formation of the pyridinium salts the vitrinites were the most reactive and gave similar results to those found for a series of vitrinite rich coals of various ranks. If the sporinites had a highly cross linked aliphatic structure similar to that found in Type I or Type II oil shale kerogens one would expect these exinites to be unreactive. However, they have been found to be only slightly less reactive than vitrinite. Apparently, the yields in this reaction cannot explain the difference in reactivity between sporinites and vitrinites in pyrolysis and SCT liquefaction (15), but do reflect the lower reactivity of inertinites.

A tentative conclusion is that sporinites and vitrinites of the same rank have very similar structures but vary in the mix of aliphatics and aromatics while the structures in inertinites are very different.

ACKNOWLEDGEMENTS

This work was performed under the auspices of the Office of Basic Energy Sciences, Division of Chemical Sciences, U.S. DOE under contract W-31-109-ENG-38. The authors thank K.L. Stock for the maceral separations, G.R. Dyrkacz for the petrographic analysis and helpful discussion, and W. Spackman, Penn. State University for choosing and providing the coal samples.

REFERENCES

1. G.R. Dyrkacz, C.A.A. Bloomquist, and E.P. Horwitz, Sep. Sci. Technol. 16, 1571 (1981).
2. G.R. Dyrkacz and E.P. Horwitz, Fuel 61, 3 (1982).
3. K.W. Zilm, R.J. Pugmire, S.R. Larter, J. Allan, and D.M. Grant, Fuel, 60 717 (1981).
4. R.J. Pugmire, K.W. Zilm, W.R. Woolfenden, D.M. Grant, G.R. Dyrkacz, C.A.A. Bloomquist, and E.P. Horwitz, J. Org. Geochem. (in press).

5. R.E. Winans, G.R. Dyrkacz, R.L. McBeth, R.G. Scott, and R. Hayatsu, Proceedings Inter. Conf. Coal Sci., Dusseldorf, Verlag Gluckauf, Essen, p. 22 (1981).
6. J. Allan and S.R. Larter, Proceedings of 10th International Meeting on Organic Geochemistry, Bergen, Norway (1982) (in press).
7. G. van Graas, J.W. de Leeuw and P.A. Schenck, Adv. in Org. Geochemistry 1979, A.G. Douglas and J.R. Maxwell, Eds., Pergamon Press, Oxford, p. 485 (1980).
8. H.L.C. Meuzelaar, A.M. Harper, and R.J. Pugmire (this volume).
9. P.H. Given, M.E. Peaver, and W.F. Wyss, Fuel 39 323 (1960); Fuel 44, 425 (1966).
10. A.G. Sharkey and J.T. McCartney, in "Chemistry of Coal Utilization," M.A. Elliot, Ed., Wiley-Interscience, NY p. 241 (1981).
11. R. Hayatsu, R.E. Winans, R.G. Scott, L.P. Moore, and M.H. Studier, Fuel 57 541 (1978).
12. C.M. White, J.L. Schultz, and A.G. Sharkey, Nature 268, 620 (1977).
13. D.W. Jones, H. Pakdel, and K.D. Bartle, Fuel 61, 44 (1982).
14. B.P. Tissot and D.H. Welte, "Petroleum Formation and Occurrence," Springer-Verlag, N.Y. (1978).
15. H.H. King, G.R. Dyrkacz, and R.E. Winans (submitted to Fuel).

TABLE I. Sample Characterization and Reaction Yields

Sample	Elemental Analysis							Maceral Composition			Vacuum Pyrolysis Yields				Pyridine/I ₂		Ag ₂ O Oxidation Solubles (Wt%)
	(DMF %)							%	%	%	Yields			Wt % Increase 100 C	Py I ⁺ / I ⁻		
	C	H	N	S	O ¹	Ash	Exinite				Vitrinite	Inertinite	Volatiles			Tar	
Indiana (PSOC 828) Brazil Block																	
Whole	74.3	5.9	1.5	1.0	17.3	<1.0	15.1	61.8	23.1		29.6	8.4	62.0		23.4	3.1	48.4
Exinite ²	78.6	7.5	1.1	1.6	11.2	<1.0	91.0	9.0	~0		23.3	48.4	28.3		19.4	2.6	59.0
Vitrinite	76.4	5.6	1.5	0.9	15.6	<1.0	4.0	89.8	6.2		16.3	16.9	67.8		24.8	3.3	60.3
Inertinite	77.1	5.0	1.3	0.7	15.9	<1.0	0.0	62.5	32.5		16.9	13.4	69.7		19.4	2.6	45.5
Kentucky Upper Elkhorn #3 (PSOC 1103)																	
Whole	72.0	5.6	1.4	2.3	18.7	<1.0	7.4	74.2	18.4		12.2	24.5	63.3		28.6	3.8	50.3
Exinite ²	80.9	6.4	1.5	1.1	10.1	<1.0	45.5	49.6	4.9		14.8	35.2	50.0		25.8	3.4	41.5
Vitrinite	80.4	5.6	1.8	1.0	11.2	<1.0	2.5	92.5	5.0		20.2	22.7	57.1		28.8	3.9	62.5
Inertinite	70.9	3.8	1.2	8.8	15.3	?	1.5	16.2	82.3 ³		8.3	5.9	85.9		14.1	1.8	45.8
Illinois No. 2																	
Whole	73.1	5.3	1.3	2.2	18.1			88.6							37.5	5.0	
Vitrinite	73.9	5.3	1.1	1.6	18.1	<1.0		>95			18.3	5.4	76.3				
Inertinite ⁴	79.3	3.2	.5	4.0	13.0	4			>90		10.7	1.8	87.5				

¹By difference; ²Mostly sporinite; ³Contains 49.8% pseudo-vitrinite; ⁴Mostly fusinite, hand picked; pyrolysed at 500°C.

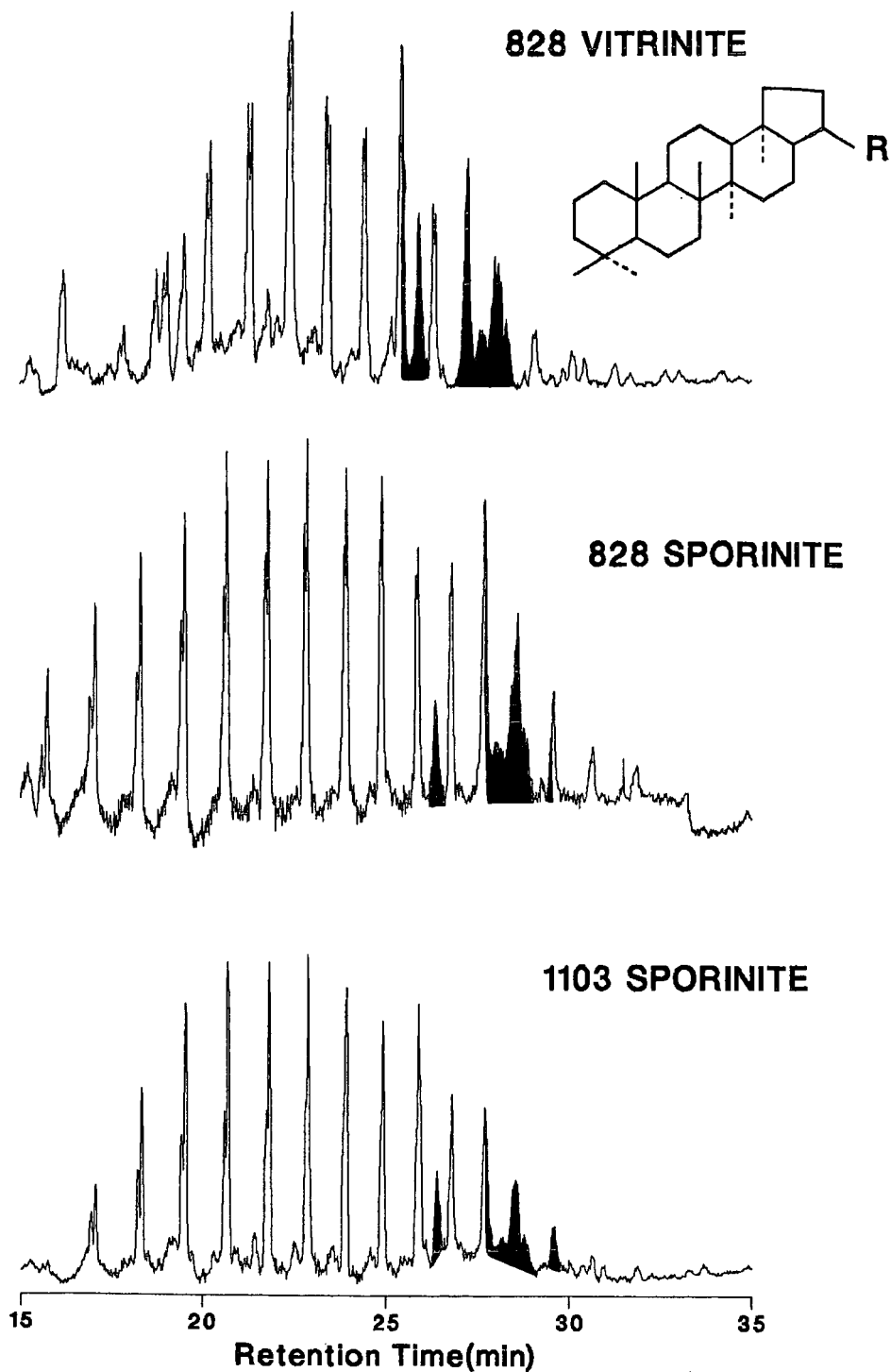


Figure 1. Partial gas chromatograms of vacuum pyrolysis tars. The shaded peaks are compounds derived from triterpenes.

THE INFLUENCES OF MACERALS ON THE HYDROGEN-DEUTERIUM EXCHANGE REACTION BETWEEN TETRALIN AND DIPHENYLMETHANE

Chol-yoo Choi and Leon M. Stock

Department of Chemistry
University of Chicago
Chicago, Illinois 60637

INTRODUCTION

The concept that free radical reactions predominate during coal dissolution reactions is quite widely accepted (1). Recent findings concerning the selective and reversible abstraction reactions of hydrogen atoms from tetralin by radicals formed during the thermal decomposition of Illinois No. 6 coal at 400°C support this interpretation (2). The fact that weak organic acids and bases have only a modest influence on the rates of the exchange reactions of aromatic, aliphatic, and benzylic hydrogen atoms under these conditions whereas compounds such as benzyl phenyl ether, benzyl phenyl sulfide, thiophenol, the BDPA radical, anthraquinone, anthrone, tetracene, and acridine actively promote the benzylic exchange reactions are also in accord with the view that radical processes dictate the outcome of coal dissolution (2). Indeed, benzyl phenyl sulfide and thiophenol significantly enhance the rate of dissolution of Illinois No. 6 coal (3). The interactions between coals and donor molecules such as tetralin have been examined in several laboratories to improve the understanding of these reactions (2,4-6). However, no information concerning the reactivity of coal macerals in such situations has been available. Accordingly, we have compared the influences of maceral concentrates of some selected coals on the exchange reactions between tetralin-d₁₂ and diphenylmethane.

EXPERIMENTAL PART

The macerals used in this study were obtained from G. R. Dyrkacz and R. E. Winans of the Argonne National Laboratory. Some of the samples were prepared by density gradient centrifugation and others were prepared by float-sink techniques. The coal particles in all these samples were milled to three micron diameter and the separations were conducted in the presence of a surface active agent, polyoxyethylene (23) lauryl ether, in cesium chloride solutions (7).

The exchange reactions were conducted using a degassed solution of diphenylmethane (0.376 mmole) and tetralin-d₁₂ (0.376 mmole) and the maceral material (25 mg) in a sealed glass vessel under an argon atmosphere at 400°C. The reactions were carried out for different times depending upon the reactivity of the maceral.

The products were isolated and analyzed using high field nmr spectroscopy as previously described (2). However, the macerals incorporate deuterium during the reactions and the change in the deuterium content of tetralin-d₁₂ is emphasized in this report rather than the degree of incorporation of this isotope into diphenylmethane. Control experiments indicated that neither polyoxyethylene (23) lauryl ether nor cesium chloride altered the rate of the exchange reactions between tetralin-d₁₂ and diphenylmethane.

The compositions of the macerals were determined by G. R. Dyrkacz. As already reported (7), the PSOC 106 maceral concentrates were greater than 90% pure. For PSOC-828, separation I, it was found that the exinite concentrate contained 91% exinite and 9% vitrinite; the vitrinite concentrate contained 4% exinite, 90% vitrinite and 6% inertinite; the inertinite concentrate contained 62.5% vitrinite and 32.5% inertinite. For PSOC-1103, separation II, it was found that the exinite concentrate contained 46% exinite, 50% vitrinite, and 5% inertinite; the vitrinite concentrate contained 3% exinite, 93% vitrinite and 5% inertinite; the inertinite concentrate contained 2% exinite, 16% vitrinite, 33% inertinite, and 50% other material--either semifusinite or pseudovitrinite. The data provided by the sample bank strongly suggest that this material is semifusinite.

RESULTS AND DISCUSSION

The exchange reactions of the macerals isolated from two hvB bituminous coals, PSOC-106 and PSOC-828, are presented in Tables 1 and 2, respectively.

Table 1. The influence of the macerals from PSOC-106 on the deuterium-hydrogen exchange reaction of tetralin-d₁₂ and diphenylmethane at 400°C^a

Maceral (mg)	Deuterium Content of Tetralin (%)		
	Aromatic Positions	Benzylic Positions	Aliphatic Positions
None	95.1	92.3	92.3
Exinite (25.3)	94.7	79.6	89.1
Exinite (24.9)	95.6	83.8	90.1
Vitrinite (25.6)	95.4	84.9	89.9
Vitrinite (25.4)	95.3	84.2	89.7
Inertinite (25.1)	95.1	86.7	89.3
Inertinite (25.2)	94.7	86.9	88.6

^aDiphenylmethane (0.376 mmole) and tetralin-d₁₂ (0.376 mmole) were reacted for 60 minutes in the presence of these macerals. The tetralin-d₁₂ used in these experiments contained 96.1, 96.8 and 93.7% deuterium at the aromatic, benzylic, and aliphatic positions.

Table 2. The influence of macerals from PSOC-828 on the deuterium-hydrogen exchange reaction of tetralin-d₁₂ and diphenylmethane at 400°C^a

Maceral (mg)	Deuterium Content of Tetralin (%)		
	Aromatic Positions	Benzylic Positions	Aliphatic Positions
Experimental Series A			
None	94.7	91.3	93.0
Demineralized coal (25.6)	94.1	82.5	90.8
Exinite (25.4)	94.3	75.9	90.6
Vitrinite (25.4)	94.1	80.0	90.9
Inertinite (25.8)	94.7	82.4	90.3
Experimental Series B			
None	95.7	92.2	92.7
Raw whole coal	95.0	75.8	89.2
Demineralized coal	95.0	80.2	89.6
Exinite	94.9	80.0	89.1
Vitrinite	95.5	81.1	88.8
Inertinite	94.9	81.5	87.5

^aDiphenylmethane (0.376 mmole) and tetralin-d₁₂ (0.376 mmole) were reacted for 60 minutes in the presence of these macerals. The tetralin-d₁₂ used in these experiments contained 96.1, 96.8 and 93.7% deuterium at the aromatic, benzylic, and aliphatic positions.

The exchange reactions of the macerals isolated from different coals are presented in Table 3.

Table 3. The influences of macerals isolated from different coals on the deuterium-hydrogen exchange reaction of tetralin-d₁₂ and diphenylmethane at 400°C ^a

Source of Maceral (mg)	Deuterium Content of Tetralin (%)		
	Aromatic Positions	Benzylic Positions	Aliphatic Positions
Experimental Series C, Vitrinites			
None	94.7	91.7	92.4
PSOC-828, separation I, (25.3)	94.3	81.5	89.1
PSOC-828, separation II (25.3)	93.9	76.3	87.8
PSOC-1103, separation I (25.1)	93.9	79.2	87.4
PSOC-1103, separation II (25.4)	93.5	77.9	88.1
Illinois No. 2, undemineralized (25.2)	94.1	78.7	90.2
Illinois No. 2, demineralized (25.2)	94.0	78.0	89.5
Experimental Series D, Exinites			
PSOC-828, separation I (25.1)	94.7	78.0	89.2
PSOC-828, separation II (25.1)	93.9	78.4	88.6
PSOC-1103, separation II (25.0)	94.1	77.9	87.4
Experimental Series E, Inertinites			
PSOC-828, separation I (25.4)	94.9	81.7	89.7
PSOC -828, separation II (25.4)	94.5	80.8	88.9
PSOC-1103, separation II (25.2)	94.3	76.5	89.4

^aDiphenylmethane (0.376 mmole) and tetralin-d₁₂ (0.376 mmole) were reacted for 60 minutes in the presence of these macerals. The tetralin-d₁₂ used in these experiments contained 96.1, 96.8 and 93.7% deuterium at the aromatic, benzylic, and aliphatic positions.

Collins and his coworkers reported that Illinois No. 6 coal reduced benzophenone to diphenylmethane (8,9). We have used this reaction to assay the reactivities of the macerals. The results are summarized in Table 4.

Table 4. The effectiveness of macerals isolated from different coals for the reduction of benzophenone at 400°C for 60 minutes ^a

Reducing Agent (mg)	Reduction (%)
Experimental Series F, PSOC-828, Separation I	
Tetralin (51)	1.0
Demineralized whole coal (5.2)	2.0
Exinite (5.2)	3.6
Vitrinite (5.1)	2.1
Inertinite (5.1)	1.9
Experimental Series G, PSOC-1103, Separation II	
Tetralin (51)	1.2
Demineralized whole coal (5.8)	3.9
Exinite (5.7)	3.5
Vitrinite (5.6)	3.2
Inertinite (5.8)	1.5

^aThe reaction solutions in glass vessels were degassed prior to the introduction of argon and sealing.

The highly purified macerals obtained from PSOC-106 selectively enhance the rate of the exchange reaction at the benzylic position of tetralin-d₁₂. The order of reactivity, exinites > vitrinites > inertinites, is clearly established for the macerals of this coal. The macerals also enhance the exchange reactions at the aliphatic positions of tetralin, but to a lesser degree. No significant exchange occurs at the aromatic positions of tetralin or diphenylmethane under the conditions of these experiments. It is notable that the ratio of benzylic to aliphatic exchange decreases as the degree of benzylic exchange decreases. The finding is compatible with the view that the radicals produced from the macerals of lesser reactivity, the inertinites in this instance, are less selective.

The observations for the exchange reactions of the somewhat less pure macerals obtained from PSOC-828 and PSOC-1103 have some features in common with the results for the pure macerals of PSOC-106. In all cases, the reaction occurs selectively at the benzylic positions. In addition, the same reactivity sequence, exinite > vitrinite > inertinite, is also observed for PSOC-828. However, the differences in reactivity are somewhat less sharply defined, possibly because the inertinite concentrate contains a large amount of vitrinite. In contrast, the inertinite fraction obtained from PSOC-1103 exerts a greater accelerating influence on the exchange reaction than does the vitrinite obtained from the same coal. Analytical data indicate that this inertinite fraction is especially rich in sulfur. Consequently, the high reactivity is not unexpected (3).

The results obtained in the reduction of benzophenone, although not without anomalies, are more regular than the results obtained in the exchange reactions. The reactivity sequence, exinite > vitrinite > inertinite, is observed for both PSOC-828 and PSOC-1103. Moreover, the inertinite concentrates from these coals are both moderately more reactive than tetralin.

This preliminary series of observations reveal that there are differences in the hydrogen donor capacity of the different macerals obtained from three different coals, however, the differences in reactivity in the test reactions used in our study are not highly pronounced.

ACKNOWLEDGEMENT

We are indebted to G.R. Dyrkacz and his collaborators and to R.E. Winans and K.L. Stock for the preparation of the macerals used in this study. The research was supported by a contract (DE-AC22-80PC30088) from the Department of Energy. The whole coal samples were provided by W. Spackman from the Penn State Coal Bank.

REFERENCES

1. Whitehurst, D. D., Mitchell, T. O. and Farcasiu, M. "Coal Liquefaction," Academic Press, New York, 1980
2. King, H. H. and Stock, L. M. Fuel, 1982, 61, 257
3. Huang, C. B. and Stock, L. M. Am. Chem. Soc., Div. Fuel Chem., Preprints 1982, 27(3-4), 28
4. Franz, J. A. Fuel, 1979, 58, 405
5. Ratto, J. J., Heredy, L. A. and Skowronski, R. P. Am. Chem. Soc. Div. Fuel Chem., Preprints 1979, 24(2), 155
6. Cronauer, D. C., McNeil, R. I., Young, D. C. and Ruberto, R. G. Fuel 1982, 61, 610
7. Dyrkacz, G. R., and Horwitz, E. P. Fuel, 1982, 61, 3
8. Collins, C. J., Benjamin, B. M., Raaen, V. F., Maupin, P. H. and Roark, W. H. "Organic Chemistry of Coal", (Ed. J. W. Larsen), Am. Chem. Soc., Washington DC, 1978, p. 165
9. Raaen, V. F. and Roark, W. H. Fuel, 1978, 57, 650

Effect of Thermal Alteration on Petrographic
Constituents of the Hanna No. 1 Coal

F. J. Rich
Department of Geology and Geological Engineering
South Dakota School of Mines and Technology
Rapid City, South Dakota 57701

A. D. Youngberg
U. S. Department of Energy,
Laramie Energy Technology Center
P.O. Box 3395, University Station
Laramie, Wyoming 82071

INTRODUCTION

The United States Department of Energy, Laramie Energy Technology Center, (LETC) has conducted numerous underground coal gasification (UCG) experiments. DOE recognizes the great potential value of UCG as a means of extracting energy from coal beds which cannot otherwise be utilized. Many beds are too deeply buried to be strip-mined, or are unsuitable for underground mining, yet constitute a vast energy reserve. We are currently developing UCG technology which should lead to an energy- and cost-efficient means of utilizing such coal beds.

LETC has chosen the Hanna No. 1 coal for experimental UCG work. The Hanna No. 1 lies within the Paleocene Hanna Formation and is confined to the Hanna Coal Basin of Wyoming (Figure 1). The No. 1 coal has been classified as a high-volatile C bituminous coal (1).

Various approaches have been used to improve the efficiency of the UCG process at the Hanna site. While these include proper installation and use of surface facilities, LETC personnel have also recognized the need for a complete understanding of the coal itself. Through careful analysis of the coal, improved systems for conversion to high quality gaseous fuel can be designed. Various types of analyses have been performed on samples of altered and unaltered coal and carbonaceous shales from the Hanna site. This report details the results of one aspect of those analyses.

PURPOSE OF THE STUDY

The purpose of the study has been to construct a geothermometer based upon visible thermal alterations in the organic constituents of Hanna No. 1 coal and carbonaceous shale samples. Youngberg, at LETC, and Rich, at the South Dakota School of Mines and Technology (SDSM&T) agreed that a correlation might be made between discrete alteration temperatures and unique petrographic compositions produced by alteration. If such a correlation could be made, then samples of coal and/or carbonaceous shale taken from UCG sites could be observed microscopically and determinations made as to the maximum temperatures to which the sediments had been subjected. The organic constituents of the samples, termed macerals, were observed, described, and quantified as changes occurred in their appearances during heating at progressively higher temperatures.

LABORATORY METHODS

Sample Preparation

Crushed bulk samples of coal and carbonaceous shale from the Hanna 170 sample site were sent to SDSM&T. One sample from 277-278 feet depth was chosen for a low ash sample (12.7% dry basis), while the sample interval 279.7-280.7 feet was

chosen for a high ash sample (63% dry basis). A third sample interval, 284.2-285.2 feet was added to the work schedule about midway through the project. Its unusual petrographic composition indicated it might actually perform better as an indicator of thermal alteration than the original samples.

Five gram samples were placed in a previously weighed crucible, and their combined weight was recorded. The furnace, meanwhile, had been heated to the desired temperature and thoroughly flushed with helium. Helium was chosen because it is totally inert and would not cause alterations in the samples in and of itself. Heating was done at 50°C intervals between room temperature (~20°C) and 600°C.

After being heated for 1 hour, the crucible was removed from the furnace as quickly as possible and weighed to record any weight change. Each sample was mixed immediately with APCO adhesive #5823. This is a low viscosity epoxy-type embedding medium which is commonly used for coal pellet preparation. The mixture of coal or shale and epoxy was divided between two steel 1-inch internal diameter steel molds, and compressed at 7000 psi for 2 minutes. After each sample hardened (~18 hours) it was labeled, then ground and polished on a Jarret Automatic Grind-Polisher.

Furnace Construction

The furnace apparatus consisted of two Parr oxygen bombs connected by a length of teflon-lined steel mesh hose (Figure 2). Only one bomb was used as a furnace. The furnace bomb was wrapped with Samox-insulated heating tape, which was then covered with several windings of Glaspun fiberglass insulating tape. The heating tape was plugged into a variable transformer which provided current for heat generation.

The lid of a Parr oxygen bomb is equipped with several fixtures, including one-way gas valves which allow flow either into or out of the bomb, and two electrical terminals which, under ordinary oxygen bomb operation, provide a heat source for sample ignition. The inlet gas valve on the furnace bomb was connected to a helium tank, while the exit valve was connected to the steel mesh hose. The hose was also connected to the second bomb, as previously mentioned. The stream of helium, then, flowed into the furnace bomb, out through the hose, and into the second bomb. From there, gases were exhausted into a fume hood. The second bomb served as a barrier to atmospheric gases which might have accidentally entered the furnace bomb, and therefore helped to prevent unwanted or dangerous combustion of samples.

One of the two electrical terminals in the furnace bomb lid was removed, and a thermocouple inserted in its place. The thermocouple was wrapped with fiberglass insulation to provide a tight seal against the air outside the bomb. The end of the thermocouple was inserted to a level just above and to the side of the crucible (Figure 2) in order that the heat sensor would measure the furnace temperature at the sample location within the bomb. Accurate temperature monitoring was provided by an Omega digital centigrade thermometer which was attached to the thermocouple.

The crucible was placed within a circular loop of wire which is designed to hold more conventional oxygen bomb samples. The crucible rested in about the middle of the furnace chamber and was, presumably, heated evenly from all sides.

A typical sample run consisted of the following steps:

1. heating of furnace bomb to preselected temperature
2. flushing of both bombs with helium
3. recording of sample weight

4. insertion of crucible into furnace bomb
5. securing furnace bomb lid
6. heating in a helium stream for 1 hour
7. removal of furnace bomb lid and sample
8. weighing of sample
9. immediate mixing of sample with epoxy
10. pellet pressing and polishing

Sample Analysis

Methods of analyzing polished pellets, or briquettes of coal are fairly well established. Stach (2) presents a concise review of techniques. The method of microscope analysis employed in this studied involved incident illumination of polished pellet surfaces and observation at 500 X magnification in oil immersion. Blue-light (actually blue-and ultraviolet wavelengths) was employed initially, though one typically observes samples using incident "white" light. Such "white" light analyses were provided by LETC, however, and so were not duplicated by Rich for unheated samples. The average maceral compositions of 108 unaltered samples of Hanna No. 1 coal are shown in Table 1.

TABLE 1. Average Maceral Composition (mineral-matter free basis)
of 108 Unaltered Coal Samples from the Hanna UCG site (1).

<u>MACERAL GROUP</u>	<u>VOLUME %</u>	<u>MACERAL</u>	<u>VOLUME %</u>
Vitrinite	91.8	Vitrinite	90.3
		Pseudovitrinite	1.5
Liptinite (Exinite)	6.1	Exinite	5.5
		Resinite	0.6
Inertinite	2.1	Semi-Fusinite	1.0
		Semi-Macrinite	0.1
		Fusinite	0.3
		Macrinite	0.1
		Micrinite	0.5
		Sclerotinite	0.1

The application of blue-light was done at first merely to see how many of the macerals in the Hanna 170 samples would fluoresce. Incident blue-light causes liptinite macerals (waxes, resins, spores, etc.) to fluoresce brightly, especially in low-rank coals. As the liptinites fluoresce they can be easily identified and quantified.

Sample surveys revealed a particular type of liptinite, exudatinitite, to be unusually common in the Hanna 170 core samples. Exudatinitite is a mobile or semi-mobile oil- or resin-like liptinite which has been recognized only in recent years (3). It occupies open spaces within the coal, and therefore tends to be found in fractures or

the lumens of coalified cells. Exudatinites in the Hanna 170 samples is especially common in structured woody tissue (telinite) and fungal bodies (sclerotinites). Inasmuch as exudatinites is rather mobile, and may actually migrate out of samples into the immersion oil (4) Rich decided to emphasize exudatinites analyses. The rationale was that, if any substances in the Hanna samples would react quickly to thermal alteration, exudatinites would certainly be among them. Exudatinites is confidently identified only in blue-light, as it fluoresces brightly, but is nearly invisible in "white" light. In view of those facts, and because exudatinites is believed to be of great potential value in geothermometry, Rich concentrated on blue-light analyses.

Two pellets from each sample interval were counted to determine relative abundances of macerals. Each pellet was attached to a glass slide with modeling clay and pressed onto the clay so that the observed surface lay parallel with the microscope stage. Counts were performed along parallel transects which did not overlap. Pellets were moved laterally by discrete units so that no adjacent fields of view overlapped. One point was counted per field of view, that point lying at the intersection of an ocular cross-hair reticle. Five hundred points were counted per pellet, and both pellets per sample were observed, providing 1000 points per sample.

TABLE 2
CHANGES IN LIPTINITE COMPOSITION FOR
SAMPLES FROM 277-278 FEET

<u>Temperature°C</u>	<u>% Liptinites</u>	<u># Exudatinites</u>	<u># Liptodetrinite & Bituminite</u>	<u># Exinite</u>
19	4.4	10	17	10
50	4.9	12	22	8
100	3.6	14	14	4
150	2.8	8	8	5
200	3.7	8	22	5
250	4.0	5	17	5
300	2.8	1	13	6
350	1.0	1	7	0
400	0.0	0	0	0

TABLE 3
CHANGES IN LIPTINITE COMPOSITION FOR SAMPLES
FROM INTERVAL 284.2-285.2 FEET

<u>Temperature°C</u>	<u>% Liptinites</u>	<u># Exudatinites</u>	<u># Liptodetrinite & Bituminite</u>	<u># Exinite</u>
21	7.7	1	58	10
50	8.5	3	67	9
100	11.5	4	87	12
150	9.3	7	68	14
200	8.3	4	69	5
250	8.5	2	67	7
300	5.2	1	38	8
350	0.8	0	6	2
400	0.0	0	0	0

RESULTS

Tables 2 and 3 illustrate several of the changes which took place during heating of samples from the 277-278 and 284.2-285.2 foot levels respectively. The following observations may be made:

- 1) In samples from both levels there was a gradual decrease in percentages of total liptinites as temperatures increased.
- 2) At both sample intervals, fluorescence essentially ceased at 400°C.
- 3) Reaction vesicles developed within vitrinite particles between 250-300°C. Vitrinite which contained spores or pollen, resin bodies, etc. became especially vesicular. Exudatinite showed distinct reactivity with consequent evacuation from sclerotinite bodies and interstices among crystals in pyrite framboids. Cracks developed in vitrinite.
- 4) Between 300-350°C vitrinite became obviously cracked and vesicular. Resinites clearly showed alteration rims as they reacted.
- 5) Between 350-400°C vitrinite became increasingly vesicular, with vesicle size and abundance increasing. Glassy or pitchy appearing deposits occurred in many vesicles. Exudatinite and resinite nearly vanished.
- 6) Within the 400-500°C range reflectivity of vitrinite particles appeared to be much more uniform. Resinite, exinite, cutinite, etc. were no longer visible in either "white" or blue light.
- 7) At 500-600°C, every coal particle developed a multitude of vesicles, and many were intensely cracked, almost brecciated. Coal particles were of uniform color and composition except for the vesicles and cracks.

Samples from the 279.7-280.7 foot interval were not point counted in blue light. The abundant clay particles were filled with detrital liptinites and were saturated with bituminite. Bituminite is another semi-mobile maceral, similar in some respects to exudatinite, which frequently infiltrates the layers of clay minerals. It thus causes the clays and interstices among clay particles to fluoresce. It is almost impossible to get an accurate quantification of bituminite in such clayey samples as virtually everything fluoresces, yet clearly the samples are not pure bituminite. Alteration in shale samples proceeded as listed for the other samples, however.

DISCUSSION AND CONCLUSIONS

Distinct petrographic changes did take place in the Hanna No. 1 samples as they were heated. Decreasing abundances of fluorescence macerals, increasing vesicularity and cracking in vitrinites, and eventual elimination of all macerals except vitrinite can be correlated with temperature ranges. It should, then, be feasible to take samples of carbonaceous shale and coal from UCG burn sites and determine the thermal gradient away from the sites.

This work has also shown that macerals in the Hanna No. 1 coal react at quite different rates when heated. Liptinites are altered before vitrinites and intertinites, though eventually all the macerals become involved in the physical alterations. The fact that liptinites react earlier than vitrinites may carry important implications as far as maintaining optimum gas composition and production are concerned.

Liptinites, for example, are enriched in hydrogen as compared to the other maceral groups. As liptinites decompose thermally, then, one would expect gases with a high hydrogen/carbon ratio to be produced. In a coal, such as the Hanna No. 1 which contains an abundance of easily altered liptinites (e.g. the resinite-rich Blind Canyon seam of Utah) conversion of coal to gas could occur at a comparatively low temperature and yet yield a gaseous product enriched in hydrogen. On the other hand, coals which do not have such an abundance of liptinites might require higher conversion temperatures which would involve more vitrinite in the conversion reactions in order to produce gases with a high hydrogen content.

An additional observation is that at higher temperatures, i.e., 400°C and above where particles become vesicular and fractured the reactive surface area within coal fragments is much greater than at cooler temperatures. The abundance of vesicles and the eventual brecciation of the particles should allow the coal to react more readily with hot gases within the gasification chamber. Brecciated coal particles would, of course, also allow product gases to move more readily through the coal bed than if the coal fragments were less extensively broken.

We believe the results of the work show that the most successful UCG operations will be those where careful consideration has been given to the petrographic composition of the coals. Petrography can be used both as a geothermometer and as a technique to predict coal reactivity during underground gasification.

References

1. Youngberg, A. D., 1981, Petrographic Analysis of Unaltered and Thermally Metamorphosed Coal from the Hanna, Wyoming, Gasification Area: Seventh Underground Coal Conversion Symp., Fallen Leaf Lake, Calif., Sept. 8-11, p. 402-415.
2. Stach, E., 1975, Coal Petrology: Gebruder Borntraeger, Berlin, 428 p.
3. Teichmüller, M., 1974, Über neue Macerale der Liptinit-Gruppe und die Entstehung des Micrinit: *Fortschr. Geol. Rheinld. u. Westf.*, v. 24, p. 37-64.
4. Spackman, W., A. Davis, and G. D. Mitchell, 1976, The Fluorescence of Liptinite Macerals: *Brigham Young Univ. Geol. Studies*, v. 22, pt. 3, p. 59-75.

Figure 1
Location of Hanna Basin

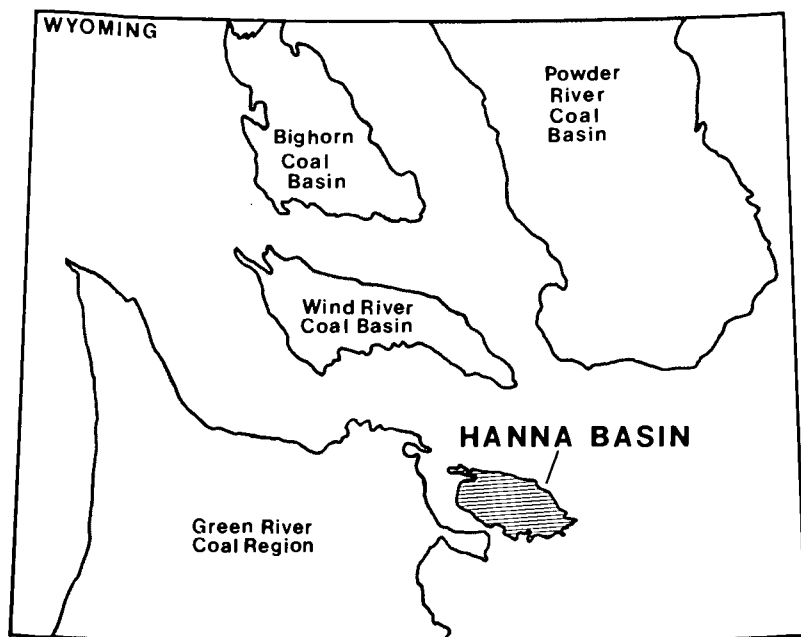
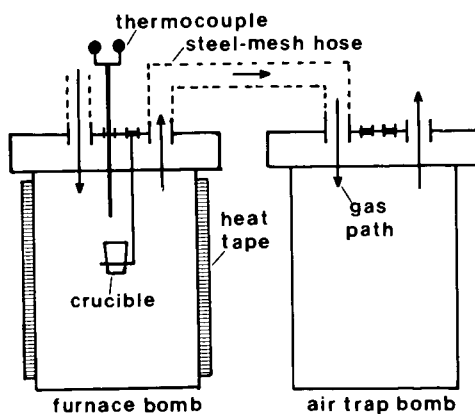


Figure 2
Bomb Assembly



HYDROUS METAL OXIDE ION EXCHANGERS AS HYDROGENATION CATALYSTS FOR DIRECT COAL LIQUEFACTION*

H. P. Stephens, R. G. Dosch and F. V. Stohl

Sandia National Laboratories, Albuquerque, NM 87185

INTRODUCTION

Interest in efficient conversion of coal to liquid fuels has encouraged exploration of promising catalytic systems for direct coal liquefaction. We have identified a group of hydrous oxide ion exchange compounds of Ti, Zr, Nb, and Ta which can be used to prepare hydrogenation catalysts by a novel synthesis route involving exchange of active metals into these compounds. Hydrous oxide ion exchange compounds have previously been investigated at Sandia National Laboratories for use in decontamination of aqueous nuclear waste (1,2) and as precursors for ceramic materials (3). A number of properties of the compounds suggested their use as substrates for catalyst preparation: 1) any metal or mixture of metals can be atomically dispersed in the materials over a wide concentration range by a simple process; 2) the materials have high surface areas; 3) they exhibit good chemical stability; 4) solution chemistry or high temperature reactions can be used to provide active metal oxidation state control; and 5) acidity and basicity of the substrate can be modified by ion exchange.

Although these properties suggested hydrous oxide ion exchangers may exhibit wide versatility for catalyst preparation, it was not known if catalysts synthesized by exchanging ions of active metals into the material would exhibit hydrogenation activity. The purpose of the experiments reported here was to explore the hydrogenation activity of these materials for slurry phase catalysis of direct coal liquefaction. It is also possible that hydrous metal oxide ion exchangers may be used to prepare multifunctional catalysts and catalysts for other reactions such as oxidation or dehydrogenation.

EXPERIMENTAL

Preparation and Characterization of Catalysts

The titanate system, the best characterized and least expensive of the hydrous oxides, was chosen for exploratory testing. Titanate catalysts were prepared by exchanging the sodium ions of a hydrous oxide titanium compound, generically called sodium titanate (ST), with the desired metal ions in aqueous solution. ST was prepared by reacting tetraisopropyl titanate with sodium hydroxide in methanol, hydrolyzing the solution in a water acetone mixture and drying the resulting precipitate at ambient temperature under vacuum. The preparation steps may be illustrated as follows:

- (1) $\text{Ti}(\text{OC}_3\text{H}_7)_4 + \text{NaOH} \xrightarrow{\text{CH}_3\text{OH}}$ Soluble Intermediate
- (2) Soluble Intermediate $\xrightarrow[\text{H}_2\text{O}]{\text{acetone}}$ $[\text{NaTi}_2\text{O}_5\text{H}]_x$
- (3) $2[\text{NaTi}_2\text{O}_5\text{H}]_x + x\text{Ni}(\text{aq}) \longrightarrow 2x\text{Na} + [\text{Ni}(\text{Ti}_2\text{O}_5\text{H})_2]_x$

* This work supported by the U. S. Dept. of Energy, Contract No. DE-AC04-76DP00789.

A typical ST product is an amorphous fluffy powder, which contains approximately 20% residual volatile constituents, predominately water and minor amounts of alcohols. The titanates of other metals, formed by exchange of the sodium ions, were found to have the same morphology and volatile content as the starting ST material. Drying the titanates at elevated temperature resulted in loss of volatiles. Approximately 90% of the volatiles were removed at 200°C and greater than 95% were removed after heating to 400°C. X-ray diffraction and SEM work indicated that a transition from an amorphous to a crystalline form (rutile) occurs at approximately 600°C. This is supported by DTA and TGA studies, which showed a large exotherm with no corresponding weight change at the same temperature.

Surface areas and pore volumes for several titanates have been measured by nitrogen BET and adsorption-desorption techniques. Surface areas for the material ranged from 150 to 300 m²/g and the desorption pore volumes from 0.24 to 0.41 cc/g. All of the titanates had bimodal pore volume distributions similar to the distribution illustrated for Ni titanate (total pore volume = 0.31) in Figure 1. For comparison, the unimodal pore volume distribution for a Ni/Mo on alumina catalyst, Shell 324, (total pore volume = 0.44) is also shown.

Materials, Apparatus and Procedure

Liquefaction reactions were performed with Illinois No. 6 (Burning Star) coal, SRC-II heavy distillate solvent from the Ft. Lewis Pilot Plant (1:2 coal:solvent, by weight) and high purity hydrogen. Shell 324, a 2.7% Ni/13.2% Mo on alumina catalyst, currently used in integrated two stage liquefaction pilot plant studies (4), was ground to -200 mesh and used as a reference for comparison of catalytic activity. Control experiments were also performed without catalyst addition.

As a result of screening liquefaction experiments with a number of titanates, including Cr⁺³, Fe⁺³, Fe⁺², Ni⁺², Pd⁺², Mo*, Rh⁺³, Ru⁺³, Co⁺², Mn⁺² and Eu⁺³, three were chosen to test the effects of active metal, metal loading and post-preparation treatment on catalytic activity.

A randomized factorial experimental plan (3 x 2 with duplication) was used to test the effect of active metal and metal loading on liquefaction activity. For these experiments, Ni, Mo and Pd titanates with metal loadings of 1% and 10%, by weight of titanate, were used. Catalyst weight added to the reactor was adjusted so that liquefaction reactions with the 1% titanates were performed with 4 x 10⁻⁵ moles of active metal and reactions with the 10% titanates with 4 x 10⁻⁴ moles. To test the effects of catalyst post-preparation treatments, which result in loss of volatiles and surface area, and oxidation or reduction of the Ni, duplicate experiments were performed with the 10% Ni titanate heated for two hours at six conditions--300, 450 and 700°C in air and hydrogen. Reference experiments with Shell 324 were performed with the same number of moles of active metal (Ni + Mo) as the 10% loading experiments.

All liquefaction reactions were performed in 40 cm³ microreactors which were charged with 2.67 g of coal, 5.33 g SRC-II,

* Oxidation state not determined.

and powdered catalyst, pressurized to 800 psig (cold) with hydrogen, then heated to 425°C for 30 minutes and shaken at ~150 cycles/min. during the heating period. Temperatures and pressures were accurately recorded with a digital data acquisition system during the course of the experiments. Following the heating period of each experiment, the reaction vessel was quenched to ambient temperature, the resulting pressure was recorded, a gas sample was taken, and the product slurry was subsampled for analysis.

Product Analyses

Gas samples were analyzed for mole percentages of CO, CO₂, H₂S and C₁-C₄ hydrocarbons with a Hewlett-Packard 5710A gas chromatograph, which was calibrated with standard mixtures (Matheson Gas Products) of hydrocarbon gases in hydrogen. Hydrogen in the samples was obtained by difference as the remainder of the product gas mixture. The quantity of each gas produced was calculated from the mole percent in the gas sample and the post-reaction vessel temperature and pressure using an ideal gas law calculation. Hydrogen consumed during the reaction, obtained as the difference between the initial charge and hydrogen remaining after the reactor was quenched, was reported on a percent dmmf coal basis.

The reaction product slurry was analyzed for insols, high molecular weight (mw) product, intermediate mw product and low mw product by tetrahydrofuran (THF) solubility and high performance liquid chromatography (HPLC). A 0.2 g subsample was mixed with about 50 ml of THF, filtered to obtain the weight of insols, and brought to 100 ml with additional THF. Chromatograms of 5 μ l aliquots of the filtrate were obtained with a Waters Assoc. Model 6000A solvent delivery system, a 100 Å microstyrigel gel permeation column, and a Model 440 uv absorbance detector. The uv absorbance response factors for the product groups were determined using calibration samples prepared by dissolving known weights of high (~1000 g/mole), intermediate (~500 g/mole) and low (250 g/mole) mw coal-derived products obtained by preparative scale liquid chromatographic (gel permeation) separation of whole liquid product from liquefaction reactions performed under similar conditions with the same coal and solvent. Chromatogram area measurements and response factors were used to calculate the percentages of high, intermediate and low* mw products for the THF soluble product. Conversion data were calculated on a dmmf coal basis, and included corrections for the conversion of the pyrite content of the coal to pyrrhotite and the loss of volatiles, if any, from the catalyst.

RESULTS AND DISCUSSION

Previous statistical analysis of experiments with oil soluble catalysts (5) has shown that hydrogen consumption and conversion to low mw product may be used as quantitative measures of catalyst activity for coal liquefaction. Figures 2 and 3 illustrate the conversion to low mw product and hydrogen consumption for the experiment with the 1 and 10% Ni, Mo and Pd titanates without post-preparation treatments. The values represented in the figures are the averages of duplicate experiments. Standard deviations were statistically determined to be 1.4% for conversion

* % conversion to low mw product is approximately equivalent to pentane soluble product.

to low mw product and 0.13% for hydrogen consumption. As can be seen from Figures 2 and 3, the ranking for metals effect with respect to both low mw conversion and hydrogen consumption is Pd > Mo > Ni and with respect to metals loading is 10% > 1%.

Results of a two way analysis of variance were used to make a quantitative comparison of performance. The effect of active metals (1 and 10% loadings averaged), were as follows:

low mw product:

Pd (47.7%) > Mo (45.3%) > Ni (43.0%) $F = 10.8$, $P < .01$;

hydrogen consumption:

Pd (1.86%) > Mo (1.65%) > Ni (1.35%) $F = 22.4$, $P < .005$,

where F is the variance ratio and P is the probability of a chance occurrence of the result. These values may be compared with the results of experiments without catalyst addition (low mw product = 26.8% and hydrogen consumption = 0.69%) and experiments with Shell 324 (low mw product = 42.8% and hydrogen consumption = 1.88%). It was found that the 10% titanates averaged 3.2% greater conversion ($F = 10.8$, $P < 0.01$) and 0.37% greater hydrogen consumption ($F = 35.0$, $P < .005$) than the 1% titanates.

Only one post-preparation treatment of the 10% Ni titanates was found to have a significant effect on catalytic activity. Experiments with the titanate heated to 700°C in air produced a conversion of 33.6% to low mw product and had a hydrogen consumption of 0.71% which was significantly lower than the values for the other treatments ($45.2 \pm 1\%$ and $1.5 \pm 0.2\%$). X-ray diffraction analysis of the post-preparation treated materials shows formation of NiTiO_3 for only the material heated to 700°C in air. The NiTiO_3 formed probably cannot be reduced to Ni under liquefaction conditions and therefore is not available for catalysis of hydrogenation reactions. This has been supported by preliminary oxygen chemisorption experiments which show that the 700°C/air treatment produces a catalyst that has less than half the active nickel of the other materials.

Although this preliminary study was brief in its scope, the results indicate that catalysts prepared using hydrous metal oxide exchange compounds show promise for potential application to coal liquefaction processes. The initial activities of the titanates appear to be at least comparable to a commercial catalyst currently used in pilot plant liquefaction studies. Considering the versatility of the hydrous oxide ion exchangers with respect to their potential for preparation of multi-metal loadings and adjustment of substrate acidity or basicity, it is possible that these materials can be used to produce improved catalysts for direct coal liquefaction and other hydrogenation processes.

REFERENCES

1. R. G. Dosch, "The Use of Titanates in Decontamination of Defense Waste", SAND-78-0710, Sandia National Laboratories, Albuquerque, NM, June 1978.
2. R. G. Dosch, "Final Report on the Application of Titanates, Niobates, and Tantalates to Neutralized Defense Waste Decontamination - Materials Properties, Physical Forms, and Regeneration Techniques", SAND-80-1212, Sandia National Laboratories, Albuquerque, NM, January 1981.

3. D. L. Hankey, W. F. Hammetter and R. G. Dosch, "Preliminary Investigations on Microstructure Development in PZT Ceramics", Abstract, 34th Pacific Coast Regional Meeting of American Ceramic Society, October 1981.
4. H. P. Schindler, J. M. Chen, M. Peluso, and J. D. Potts, Proceedings of the Seventh Annual EPRI Contractor's Conference, Palo Alto, CA, May 1982.
5. K. P. Johnston, A. W. Lynch, H. P. Stephens, F. V. Stohl and M. G. Thomas, "Coal Liquefaction Process Research Quarterly Report for January 1 - March 31, 1982", SAND-82-1924, Sandia National Laboratories, Albuquerque, NM, October 1982.

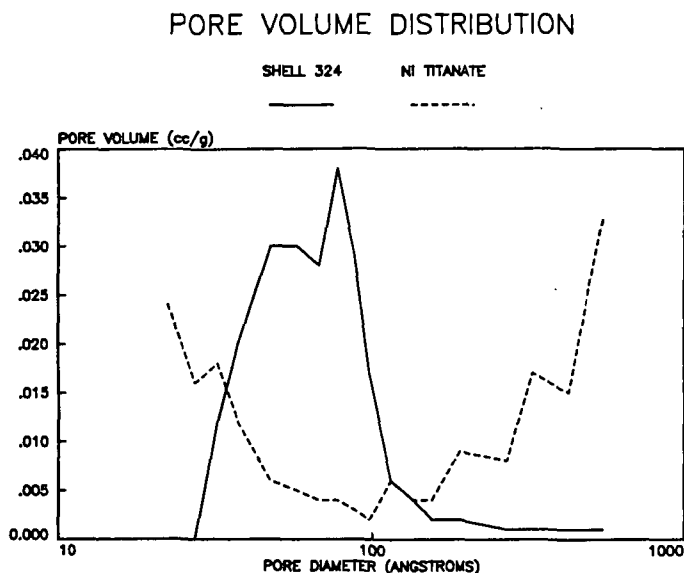


Figure 1

EFFECT OF ACTIVE METAL AND PERCENT LOADING ON CONVERSION TO LOW MW PRODUCT

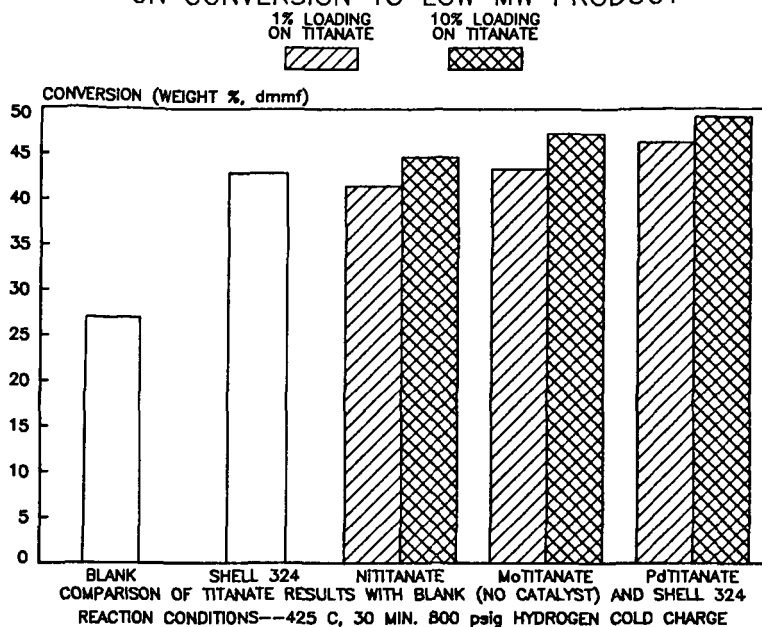


Figure 2

EFFECT OF ACTIVE METAL AND PERCENT LOADING ON HYDROGEN CONSUMPTION

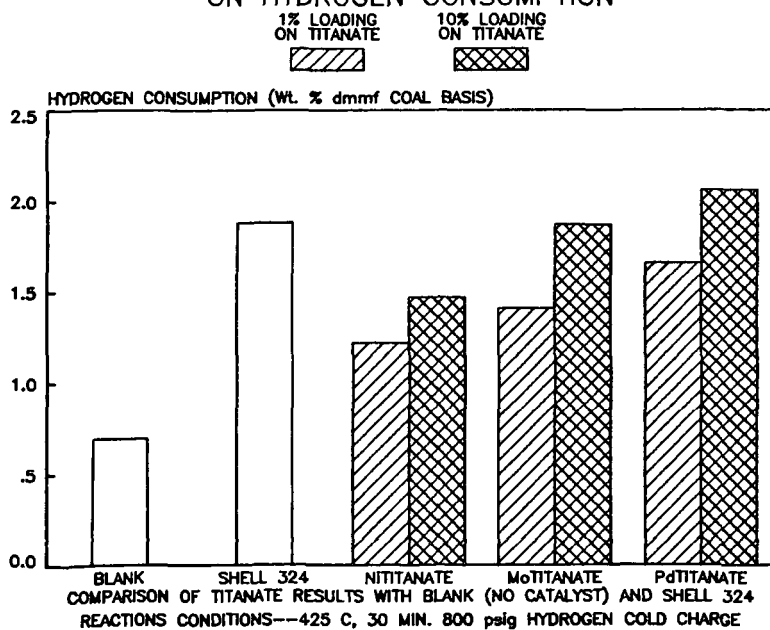


Figure 3

INTEGRATED TWO-STAGE LIQUEFACTION PROCESS - SOLVENT QUALITY EFFECTS

Eneo C. Moroni, Frank P. Burke*, Richard A. Winschel* and Bary W. Wilson**
U.S. Department of Energy, Fossil Energy/Coal Liquefaction Technology Division,
FE-34, E-338 Germantown, Washington, D.C. 20545

*Conoco Inc., Coal Research Division, Library, PA 15129

**Pacific Northwest Laboratory, Battelle, Richland, Washington 99352

Introduction

For the majority of the developed coal liquefaction processes the solvent is a portion of a selected liquefaction process stream, and not supplied from external sources, consequently a strict process control is needed to produce the required solvent balance and desired solvent quality.

Problems in maintaining both solvent balance and solvent quality has been particularly associated with the development of the SRC I process. With the introduction of the Two-Stage Liquefaction process in which SRC I is upgraded and converted to a distillate product the solvent balance does not constitute a problem anymore and the solvent quality has been improved.

Several modifications to the Two-Stage Liquefaction, which were dictated by important experimental results involving both the dissolution/hydrogenation of coal and the upgrading of the coal extract, led to a new process configuration in which first and second stages are interlocked in one integrated processing scheme. The major experimental results leading to these modifications are listed below:

- o Coal extract produced at lower operating severity than SRC I is more responsive to subsequent catalyzed reactions.^{1/}
- o Coal extracts produced at low severity can be upgraded to fuel products and a recycle process solvent of consistantly high quality.
- o Hydrogenated high boiling polyaromatics are superior hydrogen "donors" than compared to lower molecular weight tetralins.^{2/}
- o Nitrogen compounds inhibit catalytic hydrogenation of aromatics and deoxygenation of oxygen containing compounds in coal.^{3/}
- o Phenols inhibit catalytic denitrogenation of nitrogen compounds in coal or coal extracts.^{4/}
- o Heteroatom compounds, are not easily recovered since they form strong "adducts" with coals.
- o Hydrogenated polyaromatics, which also form "adducts" with coals are readily produced in the course of coal liquefaction/coal extract upgrading operations, providing a constant supply of steadily high quality recycle process solvent.

The first Integrated Two-Stage Liquefaction (ITSL) process configuration included Short Contact Time (SCT) coal extraction to maximize low severity operation in the first stage and LC-Fining using Shell 324 NiMo supported catalyst to provide extensive removal of heteroatom compounds. Further modifications of the ITSL process operating conditions were prompted by data obtained during actual

operation in the 3/4 ton coal/day ITSL process development unit at C-E Lummus, Engineering Development Center in New Brunswick, N.J., and by computed data and refining requirement as ascertained by upgrading coal-derived distillates from other processes. The major conclusions from all these sources can be summarized as follows:

- In a continuous operation the solvent fraction below 340-360°C is in vapor phase and participate little, if any, in the liquefaction of coal and also depresses the hydrogen partial pressure. Computed Vapor/Liquid equilibrium data confirm this fact.
- The -340°C fraction constitutes the most valuable refinery feedstock, being within the boiling range of gasoline, jet and diesel fuels.
- The +340°C fraction constitutes the best solvent quality for both dissolution of coal and hydrogen "shuttling."

The most recent ITSL process configuration, which is described below, attempts to exploit modifications indicated by these experimental results.

ITSL Process Flow Sheet

The current flow scheme of the ITSL operation is shown in Figure 1. Coal, hydrogen and recycle solvent (the +343°C fraction) react in the SCT reactor which is actually the SRC I preheater operated at higher outlet temperature (450°C). The gases and light oil are flashed off and the heavy oil (+343°C solvent/coal adduct) goes to the deasher. The deasher underflow containing virtually all of the ash and insoluble organic matter (IOM) goes to a vacuum flash, where the distillate portion goes overhead and combines with the deasher overflow. The ash/IOM containing flashed bottoms are drummed. Commercially this stream would go to a gasifier to generate the hydrogen for the process. The deasher overflow (cleaned +343°C solvent/coal adduct) combines with the vacuum flash overhead as feed to a continuous distillation column where the antisolvent is recovered overhead and the bottoms constitute the feed to the LC-Finer (LCFF) along with make-up hydrogen. The LC-Finer product (Total Liquid Product: TLP) is atmospherically flashed to collect the -343°C high quality product, and the +343°C bottoms are recycled to the SCT solvent pool. In this manner, the only product leaving the process is the -343°C fraction which has petroleum refinery feedstock quality superior to some petroleum crudes (Table 1).

Table 1
ITSL - PRODUCTS AND RECYCLE SOLVENT
Elemental Analysis

	<u>C</u>	<u>H</u>	<u>O</u>	<u>N</u>	<u>S</u>
Naphtha (C ₅ -177°C)	86	13	0.4	0.08	Traces
Fuel Oil (177-343°C)	88	11	0.3	0.08	0.01
Recycle Solvent (+343°C)	86	8	3.0	0.50	0.50

Phenols and nitrogen compounds are minor constituents of the process solvent compared to the level of polyaromatic hydrocarbons and they do not appear to

provide much contribution to the process solvent quality. Data examination of several ITSL recycle operations, as the coal-derived solvent replaces the hydrogenate creosote oil initial solvent, reveal the decrease of heteroatom compounds and at the same time the increase of the solvent quality. It is difficult to correlate these two experimental evidences since the more powerful the solvent becomes the more phenols and nitrogen compounds, present in the coal, are dissolved and in turn they can contribute to further the dissolution of the coal.

Bench-scale vacuum fractionation of the +343°C fraction of the recycle process solvent revealed that the heteroatom compounds, particularly nitrogen, are heavily concentrated in the +560°C distillation bottoms.

Boiling Point versus Solvent Quality (Conoco Inc.)

Relationship between boiling point and solvent quality was studied on a sample of ITSL recycle process solvent taken during steady state operation and in material balance. Twenty-two distillate fractions of ca. 100 ml. each were collected and analyzed by ¹H-NMR for proton distribution. Every third fraction was used for kinetic and equilibrium microautoclave tests.

Proton distribution of the distillate fractions are given in Table 2 along with the weight percent hydrogen for those fractions used in the microautoclave tests.

Table 2
Proton Distribution of Distillate Fractions

Fraction	Boiling Point °C	H ₂ Wt %	Condensed Aromatics	Cyclics α + β	Alkyls α + β	Alkyl γ
1	203	10.26	9.6	30.4	36.3	15.0
4	323	9.33	15.7	34.3	29.7	12.6
7	349	8.86	20.8	36.4	26.9	10.8
10	383	8.20	26.8	34.4	24.3	9.4
13	410	7.81	31.0	31.0	23.6	8.9
16	423	7.32	35.8	29.3	21.7	7.7
19	498	7.20	36.6	30.4	21.0	6.5
22	514	6.70	36.2	30.6	20.5	5.5

As the boiling point of the fractions increases the concentration of condensed aromatics increases from 8 to 39 percent. The results of the concentration of uncondensed aromatics are not shown since it decreases from 10 to 6 percent by the third fraction then remains fairly constant. The concentration of cyclic alpha and beta (naphthenic) protons, which provide one measure of donor concentration, increases for the first ten fractions, then decreases continuously to 31 percent. The concentration of alkyl alpha, beta and gamma protons which provide a measure of paraffins content decreases over the range with boiling point. Weight percent hydrogen decreases monotonically with increasing boiling point.

Microautoclave tests were carried out at 1000 psig (cold) nitrogen pressure, and are shown in Figure 2. At kinetic conditions, conversion increases sharply with boiling point to approximately 350°C (fraction 7) then the rate of increase lessens to 514°C (fraction 22).

The increase in kinetic conversion is attributed to the increase in aromaticity of the solvent with increasing boiling point as the $^1\text{H-NMR}$ data have shown. At the equilibrium conditions, conversions increase with boiling point to about 87 percent at 400°C , then decrease to 83 percent at 500°C . The equilibrium test is designed to give a measure of donor content of the solvent and the $^1\text{H-NMR}$ data on the cyclic/alkyl aliphatic proton ratio gives a relative measure of donor content in solvents with comparable hydrogen contents. The cyclic/alkyl ratio increases from 0.56 to 1.18 as the boiling points of the solvents increase. On the other hand the total hydrogen contents of the fractions decrease from 10.26 to 6.70 percent (Table 2). The shape of the curve of equilibrium test conversions vs. boiling point is caused by two opposing factors, i.e., increasing cyclic/alkyl ratio and decreasing total hydrogen content. The net effect of these opposing factors is to produce a maximum conversion at about the $375\text{--}425^\circ\text{C}$ boiling point range.

ITSL Process Solvent Components (Battelle PNL)

Total ion GCMS chromatograms show the unusual configuration of the ITSL recycle process solvent at steady state operation. The chromatogram of the deashed SCT extract which is also known as LC-Finer feed (LCFF) represented in Figure 3 shows that the solvent has donated a large portion of its hydrogen to the coal, as few large peaks of distinguishable aromatic compounds have appeared. Among major peaks identified were phenanthrene, pyrene, chrysene and also benzo(a) pyrene and anthathrene. These compounds seem to grow dominant as the solvent recycles and its hydrogen donor quality improves. The LCFF stream is hydrotreated in the second stage LC-Finer and converted to Total Liquid Product (TLP). The GCMS chromatogram of TLP is shown in Figure 4 in which the major peaks disappear, more likely due to conversion of the parent hydrocarbons to a variety of hydrogenated derivatives, except for the pyrene peak, which is only slightly hydrogenated.

Conclusion

The peculiar behaviour of polyaromatic hydrocarbons under catalytic hydrogenation/hydrocracking condition, leads to a variety of speculative thoughts on the role of each individual variety in coal liquefaction.

On the basis of preliminary data some tentative statements and speculative thoughts are presented below with the particular objective of guiding further experimental studies on the nature of the ITSL process recycle solvent at equilibrium:

- o The ITSL equilibrium process solvent is largely constituted by a few major polyaromatic hydrocarbons and related hydrogenated moieties.
- o The possibility exists now to reproduce the ITSL equilibrium process solvent by using few model compounds, i.e., hydrogenated phenanthrenes, chrysene and perhaps pyrene and their alkyl derivatives.
- o Reacting the above model solvents of different hydrogen contents with aromatic model compounds representing coal as hydrogen acceptor e.i., anthathrene and pyrene and their alkyl derivatives, a researcher can better simulate the reaction between the actual solvent and the coal.
- o Practically all the hydrogen is very rapidly donated by the process solvent and very little, if any, via hydrogen gas. Consequently, the SCT coal extraction should not be affected by gas-slurry flow-dynamics and in turn bench-scale and scale-up operations should have excellent correlation, as one of the major differences is removed.

Acknowledgment

The authors appreciate the technical support of Dr. Harvey Schindler of The Lummus Company, Mr. John Potts of Cities Service Research and Development Company and Dr. Martin Neuworth of Mitre Corporation.

References

- 1/ This experimental evidence was independently discovered by Mobil R&D Co.- F. J. Derbyshire and D. D. Whitehurst - Private Communication.
- 2/ F. J. Derbyshire et al. "Fundamental Studies in the Conversion of Coals to Fuels of Increased Hydrogen Content" EPRI AP-2117, Project 1655-1 November 1981.
- 3/ D. O'Rear - Chevron R&D Company - Private Communication.
- 4/ E. J. Hollstein, E. J. Janoski, E. G. Scheibel, A. Schneider and A. F. Talbot, Sun Tech, Inc. Research and Development of an Advanced Process for the Conversion of Coal to Synthetic Gasoline and Other Distillate Fuels - Final Report DOE/FE 2306-23, In Print.

Figure 1
Integrated Two Stage Liquefaction PDU
Current Process Flowscheme

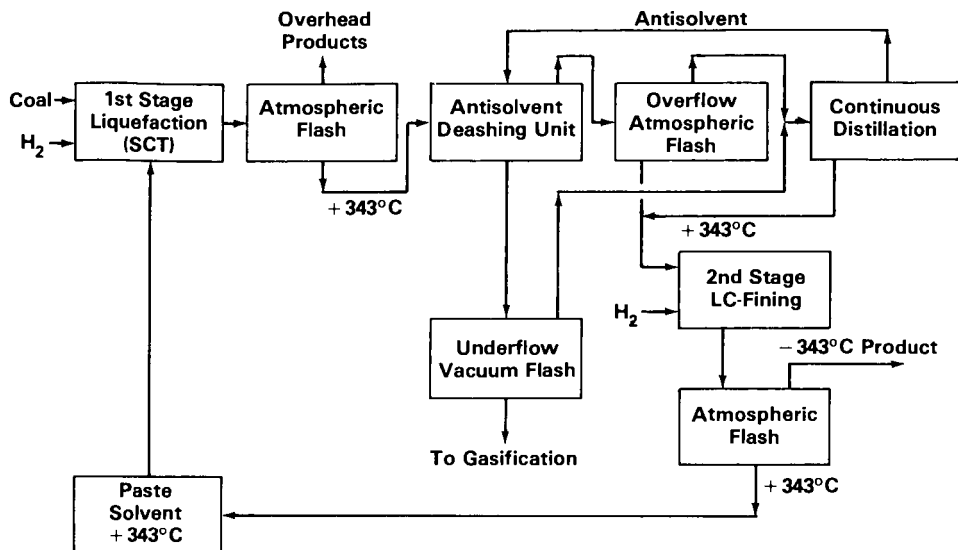


Figure 2
Microautoclave Tests with Fractions

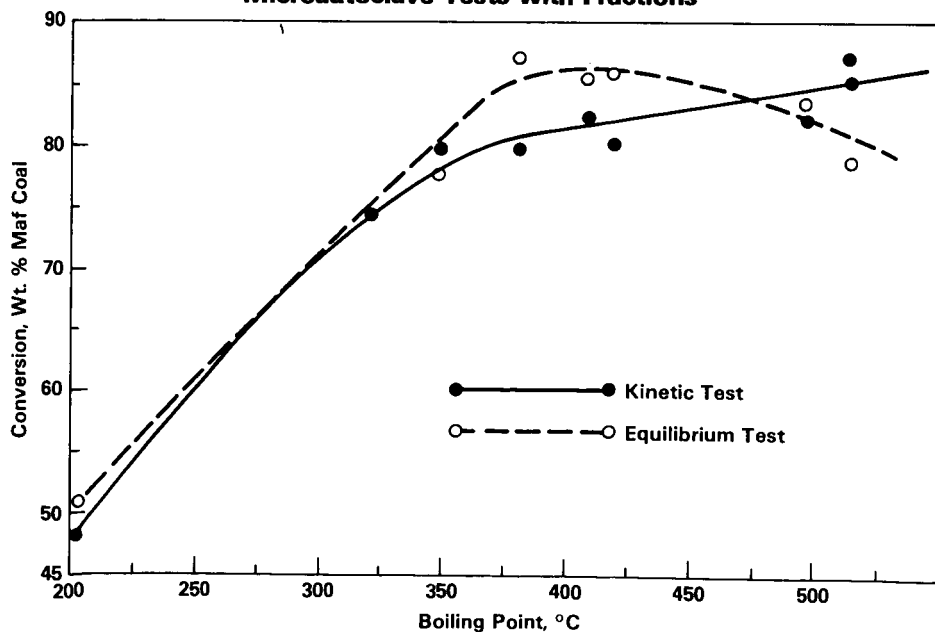


Figure 3

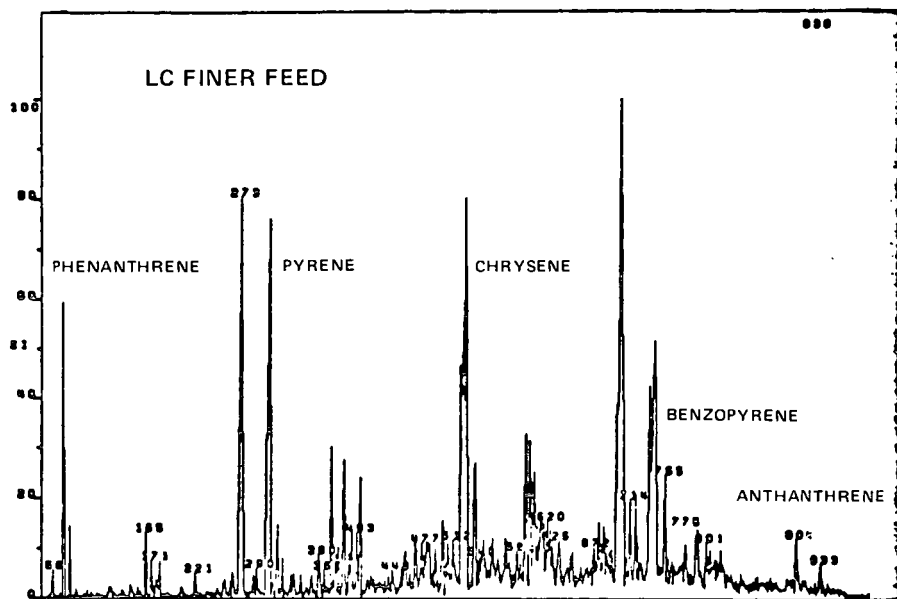


Figure 4

